

# The quark-gluon-plasma phase transition diagram, Hagedorn matter and quark-gluon liquid

Ismail Zakout<sup>1,2</sup> and Carsten Greiner<sup>2</sup>

<sup>1</sup>*Frankfurt Institute for Advanced Studies and* <sup>2</sup>*Institut für Theoretische Physik,  
Johann Wolfgang Goethe Universität, Frankfurt am Main, Germany*

(Dated: February 4, 2022)

## Abstract

In order to study the nuclear matter in the relativistic heavy ion collisions and the compact stars, we need the hadronic density of states for the entire  $(\mu_B - T)$  phase transition diagram. We present a model for the continuous high-lying mass (and volume) spectrum density of states that fits the Hagedorn mass spectrum. This model explains the origin of the tri-critical point besides various phenomena such as the quarkyonic matter and the quark-gluon liquid. The Hagedorn mass spectrum is derived for the color-singlet quark-gluon bag with various internal structures such as the unimodular unitary, orthogonal and color-flavor locked symplectic symmetry groups. The continuous high-lying hadronic mass spectrum is populated at first by the unitary Hagedorn states. Then the spectrum turns to be dominated by the colorless orthogonal states as the dilute system is heated up. Subsequently, the liquid/gas of orthogonal Hagedorn states undergoes higher order deconfinement phase transition to quark-gluon plasma. Under the deconfinement phase transition process, the color-singlet states is broken badly to form the colored  $SU(N_c)$  symmetry group. On the other hand, when the hadronic matter is compressed to larger  $\mu_B$  and heated up, the colorless unitary states (Hagedorn states) undergoes first order phase transition to explosive quark-gluon plasma at intermediate baryonic density. The tri-critical point emerges as a change in the characteristic behaviour of the matter and as an intersection among various phases with different internal symmetries. When the saturated hadronic matter is cooled down and compressed to higher density, it turns to be dominated by the colorless symplectic states. This matter exhibits the first order phase transition to quark-gluon plasma when it is heated up to higher temperature. Furthermore, when the Hagedorn states freeze out, they evaporate to the low-lying mass spectrum particles through Gross-Witten phase transition. The role of chiral phase transition is also discussed.

## I. INTRODUCTION

The phase transition diagram in the  $(\mu_B - T)$  has attracted much attention. The crucial pieces in the phase transition diagram are the existence of the tri-critical point and the discovery of quark-gluon fluid besides the other predicted phenomena such as the color-conductivity and CFL phase. The phase transition diagram persists to be proved non-trivial and very rich. The ingredient element of any investigation is the equation of state and its thermodynamics. The density of states for the hadronic mass spectrum is essential for the thermodynamic description of strongly interacting hadronic matter as well as the deconfinement phase transition to the quark-gluon plasma. The deconfined quark-gluon plasma is represented by the colored  $SU(N_c)$  symmetry group where quarks and gluons are liberated and attain the color degrees of freedom. They can also form colored quark-gluon bubbles. It is recently argued that the hadronic matter that is populated by the discrete low-lying hadronic mass spectrum exhibits Gross-Witten transition to another hadronic matter that is dominated by the continuous high-lying hadronic mass spectrum when the nuclear matter is compressed or heated up [1, 2]. The broken chiral symmetry generates a discrete mass spectrum. When the chiral symmetry is restored under the extreme conditions, we expect a continuous mass spectrum to emerge in the system. It appears that both the color and flavor sectors support the discrete and the continuous mass spectrum hadronic phase transition scenario. The discrete low-lying hadronic mass spectrum consists all the known mesons, baryons, resonances and the exotic hadronic particles which are found in the data book [3] such as  $\pi, \omega \dots$  and  $N, \Lambda, \Sigma, \Xi \dots$  etc. For instance, the non-strange discrete mass spectrum consists 76 mesons and 64 baryons. The continuous high-lying hadronic mass spectrum is the mass spectrum of the Hagedorn states and these states appear as gas/liquid of hadronic fireballs. The asymptotic continuous high-lying mass spectrum can be calculated using the canonical ensemble construction [4, 5]. These predicted states are fireballs or composite bags consisting of quarks and gluons with specific internal color and/or flavor symmetry. In order to ensure the confinement of the bag's constituent quarks and gluons and subsequently the hadronic state, the composite bag is projected to the color-singlet state (i.e. the colorless state). Hence, in QCD, it is naturally to assume that the Hagedorn states is the mass spectrum of a composite bag that is projected into color-singlet state regardless of the bag's internal symmetry. There nothing to prevent us to extrapolate the mass spectrum

of the colorless  $SU(N_c)$  state of composite bag to the colorless states of other color-flavor symmetries such as  $U(1)^{N_c}$ , orthogonal  $O_{(S)}(N_c)$  and symplectic  $Sp(N_c)$  symmetry groups. These symmetry groups are restricted to an additional unimodular-like constraint. These symmetry groups are related to each other either by the decomposition or by the reduction. In each symmetry group, the color confinement (colorless) is guaranteed by projecting only the color-singlet-state wave-function though every symmetry group represents the composite color and flavor degrees of freedom in a different way. The unimodular-like constraint is imposed in order to be consistent with QCD. This assumption of the bag's internal symmetry modification takes us to consider the possibility of the phase transition from a specific symmetry group to another one. For instance, the hadronic matter which is populated by the colorless  $SU(N)$  state bags can transmute to another matter that is dominated either by the colorless orthogonal  $O_{(S)}(N)$  state bags or by the colorless symplectic  $Sp(N)$  state bags or even by colorless  $U(1)^{N_c}$  state bags.

The effective Coulomb Vandermonde potential is induced by the symmetry group constraint that projects the bag's color-singlet state. It has been shown that the effective Coulomb Vandermonde potential is regulated in a nontrivial way in the extreme hot and dense nuclear bath. The characteristic modification of the Vandermonde potential within  $SU(N_c)$  symmetry causes the third order Gross-Witten hadronic (Hagedorn) transition [6]. The physics around Gross-Witten point neighbourhood is very rich. The emergence of new class of hadronic matter (i.e. Hagedorn states) is relevant to the tri-critical point [7]. The authors of Refs. [8, 9] have shown the existence of a critical chemical potential  $\mu_c$  such that for  $T > 0$ , the physical properties for the low-lying spectrum are unaffected by the chemical potential  $|\mu| < \mu_c$ . The Gross-Witten hadronic (Hagedorn) transition has received much attention in vast fields such as the weak-strong phase transition in AdS/CFT [10] and the search for quark-gluon plasma (see for example [11–13]).

It is reasonable to expand the quark-gluon bag's internal structure to incorporate the color, flavor and angular-momentum degrees of freedom  $(N_c, N_f, L) \rightarrow (N, \dots)$  in an appropriate configuration in order to maintain the system's internal symmetry invariance in particular under the extreme hot and dense conditions. The value  $N (\equiv N_c)$  is the number of the symmetry group Hamiltonian invariant charges (see for example [14]). The unimodular-like constraint is essential in QCD-like theory. It is considered in all the symmetry groups which are considered in the present work. The symmetry group is defined by the  $N_{fun} = N$

fundamental charges and  $N_{adj}$  of adjoint charges. The unimodular constraint reduces  $N_{fun}$  and  $N_{adj}$  to  $N_{fun} = N_{fun} - 1$  and  $N_{adj} = N_{adj} - 1$ . The  $N_{adj}$  adjoint charges are invariance only over the  $N_{fun}$  fundamental charges. The  $(N_{adj} - N_{fun})$  extra real independent parameters do not appear in the Hamiltonian and they are integrated (washed) out. The unitary ensemble  $U(N)$  has  $N_{fun} = N$  fundamental eigenvalues and  $N_{adj} = N^2$  parameters. The number of extra real independent parameters is  $N_{adj} - N_{fun} = (N^2 - N)$ . This means that the unitary symmetry group has  $N$  fundamental chemical potentials and  $N^2$  adjoint parameters. The  $N^2$  adjoint parameters are transformed (diagonalized) to depend basically only on the  $N$  fundamental chemical potentials. The redundant  $(N^2 - N)$  parameters are, subsequently, integrated out and they disappear from the resultant ensemble. The orthogonal ensemble has  $N_{fun} = N$  fundamental eigenvalues and  $N_{adj} = \frac{1}{2}N(N + 1)$  adjoint parameters. The real symmetric  $N \times N$  matrix has  $N_{adj} - N_{fun} = \frac{1}{2}N(N - 1)$  redundant real parameters and these parameters are washed away by an appropriate transformation. The unitary symmetry group can be broken and decomposed to an orthogonal symmetry group with the same number of conserved charges  $N_{fun} = N$  (or  $N_{fun} = N - 1$  when the unimodular constraint is embedded). The symmetry decomposition (breaking) from  $U(N)$  to orthogonal  $O_{(S)}(N)$  leads to  $N(N - 1)/2$  Goldstone bosons emerge as glueballs (or gluon jets) in the medium. They escape from the Hagedorn bags and enrich the medium with gluonic contents and jets. The  $N(N - 1)/2$  Goldstone bosons are identified as free colorless gluon degrees of freedom while the remaining  $\frac{1}{2}N(N + 1)$  gluons remain as the exchange interacting gluons for the  $O_{(S)}(N)$  symmetry group. The definitions of  $O_{(S)}(N)$  and other symmetry groups such as the symplectic  $Sp(N)$  symmetry group shall be reviewed below in Sec. III. On the other hand, the symplectic ensemble has  $N_{fun} = N$  eigenvalues of  $N \times N$  quaternion-real matrix and  $N_{adj} = N(2N - 1)$ . The number of redundant parameters in the symplectic symmetry group is  $2N(N - 1)$ . The (unimodular) unitary color  $U(N_c)$  symmetry group may merge with other degree of freedom such as flavor symmetry  $U(N_f)$  and the symmetry of the resultant composite transmutes to a symplectic (quaternion) symmetry group through the symmetry modification mechanism that is given by  $U(N_c) \times U(N_f) \rightarrow U(N_c + N_f) \rightarrow O(2N) \rightarrow Sp(N)$ . Hence, under the preceding assumption, there is an indication that the eventual deconfined quark and gluon matter can be reached after a chain of multi-phase processes and this argument is not that simple.

The thermodynamics of quark jets with an internal color structure has been considered

using one (or two) dimensional gas [15–19]. This model is an alternate approximation to deal the color-singlet state of quark gas. The quarks are treated as classical particles but their non-Abelian interactions are introduced by the exact Coulomb gauge potential. This model has been considered to study the order of the deconfinement phase transition. The effective potential in that model is dominated by a linear potential and it differs from the effective Vandermonde potential that emerges from the symmetry group invariance Haar measure. Furthermore, the density of states for the classical quark gas is not given in these studies.

The hadronic phase transition has been studied using the bootstrap model [20, 21]. The continuous hadronic mass spectrum is an exponentially increasing mass spectrum and it resembles the bootstrap mass density, namely,  $\rho(m) \sim c m^{-\alpha} e^{bm}$  [22–25]. The grand potential density is reduced to

$$\begin{aligned} \frac{\Omega}{V} &= -\frac{\partial}{\partial V} (T \ln Z), \\ &= -T \int_{m_0}^{\infty} dm \rho(m) \frac{\partial}{\partial V} [\ln Z(m, \beta, \dots)]. \end{aligned} \quad (1)$$

The simple and reasonable approximation is the Boltzmann gas with the canonical ensemble that is given by,

$$\begin{aligned} \ln Z &= \int d^3\vec{r} \int \frac{d^3\vec{k}}{(2\pi)^3} \Lambda e^{-\beta\epsilon(p,m,r)}, \\ &\approx V \left( \frac{mT}{2\pi} \right)^{3/2} \Lambda \exp\left(-\frac{m}{T}\right), \end{aligned} \quad (2)$$

where  $\Lambda$  is the thermodynamic fugacity and  $\epsilon(p, m, r)$  is the energy of constituent particle. For the simplicity, the free energy  $\epsilon(p, m) = \sqrt{\vec{p}^2 + m^2}$  is usually adopted. When the critical point of the deconfinement phase transition is reached, the Hagedorn mass spectrum leads to the following results: The grand potential density diverges for the exponent  $\alpha \leq 5/2$ . This means that the instant phase transition to explosive quark-gluon plasma does not exist for this class of mass spectrum. The deconfinement phase transition turns to be smooth cross-over one. On the other hand, the system likely undergoes first order deconfinement phase transition when the exponent becomes  $\alpha > 7/2$  because the grand potential density and its derivative are finite at the critical point making the grand potential density continuous and making its first derivative with respect to the thermodynamic ensemble discontinuous. When the exponent  $\alpha$  which appears in the mass spectral density runs over  $5/2 < \alpha \leq 7/2$ ,

the grand potential density becomes finite and continuous over the critical temperature and chemical potential while the order of phase transition becomes rather more difficult to be determined but not really abstruse and the system undergoes higher order deconfinement phase transition. It is evident that the value of the mass/volume power exponent  $\alpha$  plays a decisive role in determining the order and shape of the phase transition diagram. Every choice for the exponent  $\alpha$  leads to a different partition function and another distinctive physical behaviour.

The smooth phase transition has been studied using phenomenological exponents of the hadron's mass-volume spectral density which are set by inspired models [22–28]. The mass and volume bag spectral density can be reduced simply to either mass spectral density or volume spectral density for a model with an adequate approximation such as the MIT bag model with the assumption of the sharp boundary surface. The dependence of the deconfinement phase transition on the mass spectral exponent  $\alpha$  which appears in the mass spectral density, namely,  $\rho = c m^{-\alpha} e^{bm}$  for the bootstrap-like model have been studied [29]. The colorless multi-quark cluster has been considered to hint some of the puzzling results in RHIC experiments [30, 31]. The Hagedorn matter below the deconfinement phase transition is found to fit the experimental and theoretical observations [32–35]. The projection of the color-singlet state resembles Polyakov Loop approach [11–13, 36–39] where the Polyakov effective potential stems from the Vandermonde potential of a specific symmetry group and interaction. The variation of the phenomenological parameters in the Polyakov effective potential reveals the internal symmetry modification by altering the correspondent Vandermonde potential. In other words, the modification of Vandermonde potential alters the bag's internal symmetry. The QCD phase transition is considered in the context of the random matrix model [40–42]. There is a strong indication of a new class of hadronic matter above the discrete low-lying hadronic matter and below the deconfined quark-gluon plasma and this matter is identified as hadronic matter which is dominated by Hagedorn states or the quarkyonic matter [43]. It is argued that the tri-critical point that appears in the phase transition diagram is related to the existence of the predicted quarkyonic matter [7] (or equivalently the Hagedorn matter). The role of Hagedorn states in both experimental and theoretical observations have been studied extensively [44–49]. A recent survey on the importance of quarkyonic matter (i.e. Hagedorn phase) in the phase transition diagram from the experimental point of view can be found in Ref. [50]. The tri-critical point in the QCD

phase transition diagram is analysed using the lattice calculations [51, 52]. The models of clustered quarks are demonstrated to smoothen the order of phase transition (for instance see [53]). Furthermore, the Hagedorn states might play a significant role in the formation of new class of compact stars at high densities. For instance, it has been proposed that the hypothetical quark stars are made of very massive quarks rather than ordinary baryons [54].

For only the sake of simplification, we do not include the Van der Waals (excluded) volume correction in the present work. Nonetheless, the extension to include the repulsive excluded volume correction is straightforward though it requires more tedious numerical calculation. This kind of calculation has been considered in Ref. [1, 2] and the references therein where the order and the shape of the deconfinement phase transition to quark-gluon plasma have been studied extensively. It has been shown that the order and shape of the phase transition depends on the internal structures of the quark-gluon bags. Different color-flavor configurations lead to different exponents  $\alpha$  for the continuous high-lying mass spectrum (Hagedorn states). The bag's internal structure depends on several constraints which are imposed to restrict the color and flavor degrees of freedom. Since the flavor degree of freedom in the hot nuclear matter tends to be invariance even for bags with more complicated color-flavor coupling, the color confinement is maintained basically by projecting the color-singlet state. Hence, the bound state that exists through the intermediate processes is a colorless state as far the deconfinement phase transition is not reached yet.

In the present work, we study the color-singlet state canonical ensemble for the quark-gluon bag in the context of various internal symmetry groups such as unimodular-like unitary  $U(N_c)$ , orthogonal  $O_{(S)}(N_c)$  and symplectic  $Sp(N_c)$  symmetry groups as well as  $U(1)^{N_c}$ . The intermediate transmutation from the hadronic matter that is dominated by the colorless unitary fireballs to another hadronic matter that is populated by the colorless orthogonal states or the colorless symplectic states is introduced in order to demonstrate the multi-nuclear phases in the phase transition diagram and the existence of the tri-critical point. We discuss possible scenarios for the deconfinement phase transition from the colorless states of unitary, orthogonal and symplectic hadronic matter to the colored  $SU(N_c)$  quark-gluon plasma. These scenarios are relevant to the possible intermediate hadronic phases those take place below the deconfinement phase transition and the emergence of the tri-critical point.

The outline of the present paper is as follows: In Sec. II, we derive the quark-gluon grand

canonical ensemble with the color-singlet  $SU(N_c)$  state in order to be extrapolated to other symmetries. The internal orthogonal, unitary and symplectic symmetry groups with the unimodular constraint are reviewed in Sec. III. The equation of state for the nuclear matter that is dominated by the Hagedorn states is given in Sec. IV. The continuous Hagedorn mass spectra are derived for the unimodular-like unitary, orthogonal and symplectic ensembles. The role of the chiral phase transition is considered in Sec. V. Several scenarios for the deconfinement phase transition are presented in Sec. VI. Finally, the conclusion is presented in Sec. VII.

## II. THE NUCLEAR MATTER FOR THE RELATIVISTIC HEAVY ION COLLISIONS

The grand canonical partition function in the equilibrium reads

$$\begin{aligned} Z &= \text{tr} \exp \left[ -\beta H + i \sum_n \vartheta_n N_n \right], \\ &= \text{tr} \exp \left[ -\beta \left( H - \sum_n \mu_n N_n \right) \right]. \end{aligned} \quad (3)$$

The thermodynamic quantities are determined from the grand canonical partition function as follows

$$\begin{aligned} \frac{\Omega}{V} &= -\frac{\partial}{\partial V} (T \ln Z), \\ \rho_i &= \frac{1}{V} \frac{\partial}{\partial \mu_i} (T \ln Z), \\ s &= \frac{1}{V} \frac{\partial}{\partial T} (T \ln Z), \\ \frac{E}{V} &= \frac{\Omega}{V} + Ts + \mu_i \rho_i, \end{aligned} \quad (4)$$

for the grand potential density, charge density, entropy and energy density, respectively. The canonical partition function can be determined by the functional integration method. The Lagrangian construction is essential. The QCD Lagrangian for quarks and gluons is given by [55]

$$\mathcal{L} = -\frac{1}{4} F_{\mu\nu}^a F^{\mu\nu a} + \bar{\psi}_i \gamma^\mu (i D_\mu)_{ij} \psi_j, \quad (5)$$

where the covariance derivative and field strength, respectively, read

$$D_\mu = \partial_\mu + i m + i g \mathbf{t}^a A_\mu^a, \quad (6)$$



and

$$F_{\mu\nu}^a = \partial_\mu A_\nu^a - \partial_\nu A_\mu^a - gf^{abc} A_\mu^b A_\nu^c. \quad (7)$$

The quarks and antiquarks are represented by the fundamental matrices  $\mathbf{t}^a$ , while the gluons are represented by the adjoint matrices  $(T^a)_{bc} = -if^{abc}$ . The fundamental representation for  $SU(N_c)$  symmetry group has  $N_c - 1$  degrees of freedom while the adjoint representation has  $N_c^2 - 1$ . The current conservation laws read

$$\begin{aligned} j^\mu &= \bar{\psi} \gamma^\mu \psi, \\ \partial_\mu j^\mu &= 0. \end{aligned} \quad (8)$$

The total conserved baryonic charge with  $U(1)_B$  group representation is furnished by

$$\begin{aligned} Q &= \int d^3x \bar{\psi} \gamma_0 \psi, \\ &= \frac{1}{\beta} \int_0^\beta d\tau \int d^3x \bar{\psi} \gamma_0 \psi. \end{aligned} \quad (9)$$

On the other hand, the color current density is given by

$$j_\mu^a(\text{color}) = \bar{\psi} \gamma_\mu \mathbf{t}^a \psi + i (T^a)_{bc} F_{\mu\nu}^b A_c^\nu, \quad (10)$$

where both the fundamental quarks and the adjoint gluons contribute to the color current.

The conserved color charge generators are given by the time-component as follows

$$Q^a(\text{color}) = \frac{1}{\beta} \int_0^\beta d\tau \int d^3x j_0^a(\text{color}), \quad (11)$$

where

$$j_0^a(\text{color}) = \bar{\psi} \gamma_0 \mathbf{t}^a \psi + i (T^a)_{bc} F_{0\nu}^b A_c^\nu. \quad (12)$$

The canonical ensemble in the Hilbert space is given by the tensor product of the fundamental and anti-fundamental particles Fock spaces and the adjoint particles Fock space. The fundamental and anti-fundamental particles are the quarks and anti-quarks while the adjoint particles are the interaction particles which are the gluons. The partition functions for the gas of fundamental particles and the gas of adjoint particles are constructed separately and then the tensor product of their resultant Fock spaces is taken in the following way,

$$Z_{q\bar{q}g} = Z_{q\bar{q}} \times Z_g. \quad (13)$$

The partition function for quark and anti-quark gas is given by

$$Z_{q\bar{q}} = \text{tr} \left[ e^{-\beta(H - \mu Q) + i\theta_i Q_i} \right], \quad (14)$$

where  $Q_i$  are the color charges. In the functional integral procedure, the partition function is reduced to

$$Z_{q\bar{q}} = \prod_{i,\alpha} \int [id\psi_{i\alpha}^\dagger][d\psi_{i\alpha}] \exp \left[ \int_0^\beta d\tau \int d^3x \sum_{i,\alpha} \bar{\psi}_{i\alpha} \right. \\ \left. \times \left( -\gamma^0 \left[ \frac{\partial}{\partial \tau} - \mu - i\frac{\theta_i}{\beta} \right] + i\vec{\gamma} \cdot \vec{\nabla} - m \right) \psi_{i\alpha} \right]. \quad (15)$$

By adopting the imaginary time method in the thermal field theory, the straightforward integration over the Grassmann variables reduces the partition function, that is given by Eq.(15), to

$$Z_{q\bar{q}}(\beta, V) = \det \left[ -i\beta \left( \left[ -i\omega_n + \mu + i\frac{1}{\beta}\theta_i \right] - \gamma^0 \vec{\gamma} \cdot \vec{k} - m\gamma^0 \right) \right]^2, \quad (16)$$

where the sum over the Matsubara (odd-) frequencies  $\omega_n$  for fermion is performed in a proper way over the physical observable  $T \ln Z_{q\bar{q}}(\beta, V)$ . The determinant is evaluated by considering the following trick

$$Z_{q\bar{q}}(\beta, V) = \exp \ln \det \left[ -i\beta \left( \left[ -i\omega_n + \mu + i\frac{1}{\beta}\theta_i \right] - \gamma^0 \vec{\gamma} \cdot \vec{k} - m\gamma^0 \right) \right]^2. \quad (17)$$

As usual, the physical observable is determined by taking the real part as follows

$$\ln Z_{q\bar{q}}(\beta, V) \rightarrow \Re e \left( \ln Z_{q\bar{q}}(\beta, V) \right). \quad (18)$$

The partition function's explicit expression reads

$$\ln Z_{q\bar{q}}(\beta, V) = \Re e \sum_n \left( (2J+1) \text{tr} \ln \left[ \beta^2 \left( \left[ \omega_n + i \left( \mu_q + i\frac{1}{\beta}\theta_i \right) \right]^2 + \epsilon_q^2(\vec{p}) \right) \right] \right), \\ = \Re e \left( (2J+1) V \int \frac{d^3\vec{p}}{(2\pi)^3} \sum_n \ln \left[ \beta^2 \left( \left[ \omega_n + i \left( \mu_q + i\frac{1}{\beta}\theta_i \right) \right]^2 + \epsilon_q^2(\vec{p}) \right) \right] \right), \quad (19)$$

where  $\epsilon_q(\vec{q}) = \sqrt{\vec{p}^2 + m_q^2}$  and  $\mu_q$  is the flavor chemical potential. The summation over the number of states is evaluated using the standard procedure. A possible extension to include the effect of the bag's smooth boundary can be found in Refs. [56, 57]. The pre-factor

$(2J + 1) = 2$  comes from the spin degeneracy. The summation over the Matsubara (odd-) frequencies is evaluated and the result reads,

$$\begin{aligned}
T \ln Z_{q\bar{q}} &= \frac{1}{\beta} \ln Z_{q\bar{q}}, \\
&= \Re e \left( (2J + 1) V \int \frac{d^3 \vec{p}}{(2\pi)^3} \left[ \epsilon(\vec{p}) + \frac{1}{\beta} \sum_i \ln \left( 1 + e^{-\beta(\epsilon(\vec{p}) - \mu - i \frac{\theta_i}{\beta})} \right) \right. \right. \\
&\quad \left. \left. + \frac{1}{\beta} \sum_i \ln \left( 1 + e^{-\beta(\epsilon(\vec{p}) + \mu + i \frac{\theta_i}{\beta})} \right) \right] \right). \tag{20}
\end{aligned}$$

The first term is temperature independent. It leads to the divergence at zero temperature and can be renormalised in the standard way. Since, we are interested on the temperature dependent terms, the first term is trivially dropped. In the extremely hot medium, the system is supposed to take any flavor symmetry under the unitary representation. The mechanism is recognised as the flavor invariance in the extreme hot nuclear matter. Hence by the assumption that there is no specific flavor symmetry configuration is preferred, we do not need to project specific flavor symmetry. It is reasonable to believe that under extreme temperature such as the case of hadronic fireballs, the system is preferred to maintain the flavor chemical equilibrium rather than carries specific internal flavor symmetry. Under this assumption a specific flavor structure such as mesonic or baryonic Hagedorn states becomes unimportant and the classical Maxwell-Boltzmann statistics becomes satisfactory.

Nonetheless, it is still possible to maintain the flavor and  $SU(N_f)$  symmetry by considering non-strangeness mesonic and baryonic Hagedorn states at low baryonic density. When the nuclear matter is compressed to higher baryonic chemical potential, the strange mesonic and baryonic Hagedorn states emerge in the system and so on. Furthermore, it is possible to imagine that under certain extreme hot and/or dense circumstances the color and flavor symmetries are modified to reproduce either the orthogonal or symplectic symmetry. The flavor degree of freedom is introduced trivially as follows

$$\begin{aligned}
\ln Z_{q\bar{q}} &= \Re e \left( (2J + 1) V \sum_q^{N_f} \int \frac{d^3 \vec{p}}{(2\pi)^3} \sum_i \left[ \ln \left( 1 + e^{-\beta(\epsilon_q(\vec{p}) - \mu_q - i \frac{\theta_i}{\beta})} \right) \right. \right. \\
&\quad \left. \left. + \ln \left( 1 + e^{-\beta(\epsilon_q(\vec{p}) + \mu_q + i \frac{\theta_i}{\beta})} \right) \right] \right), \tag{21}
\end{aligned}$$

where  $\epsilon_q(\vec{p}) = \sqrt{\vec{p}^2 + m_q^2}$ . Only the real part is taken in Eq.(21). The resultant partition

function is reduced to

$$\ln Z_{q\bar{q}}(\beta, V) = \Re \left( (2J+1)V \int \frac{d^3\vec{p}}{(2\pi)^3} \left[ \sum_i \ln (a_{q\bar{q}}(\theta_i) + i b_{q\bar{q}}(\theta_i)) \right] \right), \quad (22)$$

where

$$\begin{aligned} a_{q\bar{q}}(\theta_i) &= \left( 1 + \cos(\theta_i) \sum_q^{N_f} \left[ e^{-\beta(\epsilon_q(\vec{p}) - \mu_q)} + e^{-\beta(\epsilon_q(\vec{p}) + \mu_q)} \right] + e^{-2\beta \epsilon_q(\vec{p})} \right), \\ b_{q\bar{q}}(\theta_i) &= \sin(\theta_i) \sum_q^{N_f} \left[ e^{-\beta(\epsilon_q(\vec{p}) - \mu_q)} - e^{-\beta(\epsilon_q(\vec{p}) + \mu_q)} \right]. \end{aligned} \quad (23)$$

The partition function for quark and anti-quark in the Fock space becomes

$$Z_{q\bar{q}}(\beta, V) = \exp \left[ (2J+1)V \int \frac{d^3\vec{p}}{(2\pi)^3} \left( \frac{1}{2} \sum_i \ln [a_{q\bar{q}}^2(\theta_i) + b_{q\bar{q}}^2(\theta_i)] \right) \right]. \quad (24)$$

The Vandermonde determinant, which appears in the invariance Haar measure, contributes to the action as an additional effective potential term. The Vandermonde effective potential term becomes soft when the color eigenvalues of the stationary condition are distributed uniformly over the entire circle  $|\theta_i| \leq \pi$ . The integral of the resultant ensemble can be evaluated trivially under such circumstances. However, this will not be the case under the extreme hot and dense conditions in particular when the color eigenvalues turn to be distributed in a narrow interval  $|\theta_i| \ll \pi$ . When the saddle points congregate around the origin rather than are distributed uniformly over the entire color circle range  $|\theta_i| \leq \pi$ , the Vandermonde effective potential develops a virtual singularity. Subsequently, the action must be regulated in a proper way in order to remove the Vandermonde determinant divergence. This regulation procedure accommodates the extreme hot and dense conditions. It is usually associated with smooth phase transition. The regulation procedure corresponds the Gross-Witten third order Hagedorn phase transition in the context of  $U(N_c)$  in the limit  $N_c \rightarrow \infty$ . The same procedure can be extended to other symmetry groups such as the orthogonal and symplectic ones. The change in the analytic solution corresponds higher order phase transition from the dilute and relatively cold hadronic matter (i.e. discrete low-lying hadronic mass spectrum phase) to the highly thermally excited hadronic matter (i.e. continuous high-lying hadronic mass spectrum phase). This kind of nuclear phase transition would not mean that the deconfinement phase transition is reached. The highly thermally excited hadronic matter is interpreted as an exotic hadronic phase that is dominated by the Hagedorn states. In the lattice theory, this is implying that the weak and strong coupling is not described by the same analytic function. This strong- and weak-coupling transition

is analogous to the phase transition from the discrete low-lying mass spectrum particles to the highly excited and massive Hagedorn states (i.e. continuous high-lying mass spectrum). The Hagedorn states are given by the mass spectrum of the color-singlet state composite (colorless) where the constituent quarks and gluons are represented by the  $SU(N_c)$  symmetry group representation and these states are hadrons [58–61]. This kind of matter should not be immediately interpreted as the deconfined quark-gluon plasma. The critical Gross-Witten point is the threshold point where the Hagedorn states emerge in the system. The internal color structure is known to be essential in the phase transition to the quark-gluon plasma [58, 59, 62–64]. The deconfinement phase transition can either take place immediately when unstable Hagedorn states are produced or as a subsequent process when the metastable Hagedorn phase eventually undergoes the phase transition to quark-gluon plasma. The Hagedorn phase may undergo multiple intermediate transitions before the deconfinement phase transition is eventually reached.

The effective Vandermonde potential plays a crucial role in the intermediate phase transition processes from the hadronic phase and quark-gluon plasma. This potential is back reacted to the heat and compression of the nuclear matter. When the invariance Haar measure is regulated, another analytical solution with different characteristic properties emerges. Hence, Vandermonde determinant is regulated in a nontrivial way and the action can be expanded over the group fundamental variables around the stationary Fourier color points up to the quadratic terms. Fortunately, the saddle Fourier color points are convened around the origin and fortunately this simplifies the problem drastically. Despite the complexity of the action due to the realistic physical situation that is involved, there will be an easy way to find the quadratic expansion around the group saddle points. The resultant integral is evaluated using the standard Gaussian quadrature over the group (i.e. color) variables. Hence, beyond the Gross-Witten point the partition function can be approximated by the quadratic Taylor expansion over the group variables. The quadratic expansion of the quark and anti-quark ensemble around the saddle points is reduced to the following Gaussian-like function

$$Z_{q\bar{q}}(\beta, V) = \exp \left[ a_{q\bar{q}}^{(0)} - \frac{1}{2} a_{q\bar{q}}^{(2)} \sum_{i=1}^{N_c} \theta_i^2 \right]. \quad (25)$$

This regulated ensemble  $Z_{q\bar{q}}(\beta, V)$  leads to a continuous high-lying mass spectrum. The

coefficients which appear in the exponential are calculated in the following way,

$$a_{q\bar{q}}^{(0)} = (2J+1)VN_c \sum_q \int \frac{d^3\vec{p}}{(2\pi)^3} \ln [1 + (e^{-\beta(\epsilon_q(\vec{p})-\mu_q)} + e^{-\beta(\epsilon_q(\vec{p})+\mu_q)}) + e^{-2\beta\epsilon_q(\vec{p})}], \quad (26)$$

and

$$\begin{aligned} a_{q\bar{q}}^{(2)} = & (2J+1)V \sum_q \int \frac{d^3\vec{p}}{(2\pi)^3} \frac{(e^{-\beta(\epsilon_q(\vec{p})-\mu_q)} + e^{-\beta(\epsilon_q(\vec{p})+\mu_q)})}{[1 + (e^{-\beta(\epsilon_q(\vec{p})-\mu_q)} + e^{-\beta(\epsilon_q(\vec{p})+\mu_q)}) + e^{-2\beta\epsilon_q(\vec{p})}]} \\ & - (2J+1)V \sum_q \int \frac{d^3\vec{p}}{(2\pi)^3} \frac{(e^{-\beta(\epsilon_q(\vec{p})-\mu_q)} - e^{-\beta(\epsilon_q(\vec{p})+\mu_q)})^2}{[1 + (e^{-\beta(\epsilon_q(\vec{p})-\mu_q)} + e^{-\beta(\epsilon_q(\vec{p})+\mu_q)}) + e^{-2\beta\epsilon_q(\vec{p})}]^2}. \end{aligned} \quad (27)$$

The chemical potential  $\mu_q$  is decomposed to  $\mu_q = \frac{1}{3}\mu_B + S\mu_S + \dots$ . From the fugacity definition, it is worth to keep in mind that  $\beta\mu_q \rightarrow \frac{1}{T}\mu_q$ . In the case of massless flavors, we have

$$\begin{aligned} a_{q\bar{q}}^{(0)} = & (2J+1) \left(\frac{V}{\beta^3}\right) N_c \sum_{q=1}^{massless} \left[ \frac{7\pi^2}{360} + \frac{1}{12} \left(\frac{\mu_q}{T}\right)^2 + \frac{1}{24\pi^2} \left(\frac{\mu_q}{T}\right)^4 \right] \\ & + (\text{massive flavors}), \end{aligned} \quad (28)$$

and

$$\begin{aligned} a_{q\bar{q}}^{(2)} = & (2J+1) \left(\frac{V}{\beta^3}\right) \sum_{q=1}^{massless} \frac{1}{6} \left(1 + \frac{3}{\pi^2} \frac{\mu_q^2}{T^2}\right) + (\text{massive flavors}), \\ \approx & (2J+1) \left(\frac{V}{\beta^3}\right) \sum_{q=1}^{massless} \frac{1}{6} \left(1 + \frac{3}{\pi^2} \frac{\mu_q^2}{T^2}\right) + (\dots), \end{aligned} \quad (29)$$

where  $(\dots)$  indicates the neglected massive flavors.

The grand canonical ensemble for the adjoint gluons can be calculated in a similar way to that one done in calculating the fundamental quark and antiquark grand canonical ensemble in the functional integral representation (see for instance Eq.(15)). For the sake of simplicity, the axial gauge is considered and the result is manifestly gauge invariant [55]. In the axial gauge, the canonical partition function for a gas of adjoint gluons reads

$$Z_g(\beta, V) = \int \prod_a \int [dA_0^a][dA_1^a][dA_2^a] \det(\partial_3) e^{S_g}, \quad (30)$$

where the action is given by

$$S_g = \frac{1}{2} \int_0^\beta d\tau \int d^3x (A_0^a, A_1^a, A_2^a) \mathbf{D}(A_0^a, A_1^a, A_2^a)^T. \quad (31)$$

By constructing the canonical Lagrangian from the Hamiltonian and then by integrating the resultant Lagrangian by parts, the operator that appears in Eq.(31) is reduced to

$$\mathbf{D} = \begin{pmatrix} \nabla^2 & -\partial_1 \partial_\tau & -\partial_2 \partial_\tau \\ -\partial_1 \partial_\tau & \partial_2^2 + \partial_3^2 + \partial_\tau^2 & -\partial_1 \partial_2 \\ -\partial_2 \partial_\tau & -\partial_1 \partial_2 & \partial_1^2 + \partial_2^2 + \partial_\tau^2 \end{pmatrix}. \quad (32)$$

Following the standard procedure in the thermal quantum field theory and the expansion over the Matsubara (even-) frequencies in the imaginary time formalism, it is possible to invert the operators to standard matrices. The canonical partition function for a gas of gluons is reduced to

$$Z_g(\beta, V) = \det(\partial_3) \times \frac{1}{\sqrt{\det(\mathbf{D})}}, \quad (33)$$

where the resultant Riemann integrals are evaluated by the Gaussian integration. The determinants for the axial gauge constraint and the action read, respectively,

$$\det(\partial_3) = \prod_a^{N_c^2-1} \det(\beta p_3), \quad (34)$$

and

$$\det \mathbf{D} = \prod_{a=1}^{N_c^2-1} \det \mathbf{D}^a. \quad (35)$$

By introducing the Fourier transform and the Matsubara (even-) frequencies, the adjoint gluon operator is reduced to

$$\mathbf{D}^a = \beta^2 \begin{pmatrix} \vec{p}^2 & -(\omega_n - i\frac{\phi_a}{\beta})p_1 & -(\omega_n - i\frac{\phi_a}{\beta})p_2 \\ -(\omega_n - i\frac{\phi_a}{\beta})p_1 & (\omega_n - i\frac{\phi_a}{\beta})^2 + p_2^2 + p_3^2 & -p_1 p_2 \\ -(\omega_n - i\frac{\phi_a}{\beta})p_2 & -(\omega_n - i\frac{\phi_a}{\beta})p_1 & (\omega_n - i\frac{\phi_a}{\beta})^2 + p_1^2 + p_3^2 \end{pmatrix}. \quad (36)$$

The straightforward calculation following the standard procedure in the thermal field theory [55] leads to

$$\ln Z_g(\beta, V) = -(2J+1)V \sum_n \int \frac{d^3 p}{(2\pi)^3} \sum_{a=1}^{N_c^2-1} \ln \left( \beta^2 \left[ \left( \omega_n - i\frac{\phi_a}{\beta} \right)^2 + \vec{p}^2 \right] \right). \quad (37)$$

The sum over the Matsubara (even-) frequencies gives the following result

$$\frac{1}{\beta} \ln Z_g(\beta, V) = -(2J+1)V \int \frac{d^3 p}{(2\pi)^3} \sum_{a=1}^{N_c^2-1} \left[ \frac{1}{2} \epsilon_g(\vec{p}) + \frac{1}{\beta} \ln \left( 1 - e^{-(\beta \epsilon_g(\vec{p}) - i\phi_a)} \right) \right], \quad (38)$$

where  $\epsilon_g(\vec{p}) = \sqrt{\vec{p}^2 + m_g^2}$  and  $m_g = 0$ . The first term inside the square bracket on the right hand side of the grand potential  $\Omega = -V \frac{\partial}{\partial V} \frac{1}{\beta} \ln Z_g(\beta, V)$  that is given by Eq.(38) is temperature independent. This term must be regulated at zero temperature and must be dropped from the thermal contribution because it has no thermal origin. The grand canonical ensemble for the gluon gas is reduced to

$$Z_g(\beta, V) = \exp \left\{ -(2J+1)V \int \frac{d^3p}{(2\pi)^3} \sum_{a=1}^{N_c^2-1} \ln [1 - e^{-(\beta\epsilon_g(\vec{p}) - i\phi_a)}] \right\}. \quad (39)$$

The adjoint eigenvalues are calculated from the nested commutation relations for fundamental eigenvalues in the Lie algebra. The adjoint eigenvalues are related to fundamental eigenvalues by the relation  $\phi_a \sim (\theta_i - \theta_j)$ . This relation diagonalized the adjoint representation and subsequently commutes with the energy Hamiltonian. The canonical ensemble for gluon gas becomes

$$\begin{aligned} \ln Z_g(\beta, V) = & -(2J+1)V \int \frac{d^3p}{(2\pi)^3} \left\{ \sum_1^{N_c} \sum_{i \neq j}^{N_c} \ln (1 - e^{-[\beta\epsilon_g(\vec{p}) - i(\theta_i - \theta_j)]}) \right\} \\ & -(2J+1)(N_c-1)V \int \frac{d^3p}{(2\pi)^3} \ln (1 - e^{-\beta\epsilon_g(\vec{p})}). \end{aligned} \quad (40)$$

The gluon partition function has no imaginary and it can be re-written as follows

$$\begin{aligned} \ln Z_g(\beta, V) = & -(2J+1)V \int \frac{d^3p}{(2\pi)^3} \left\{ \sum_{i>j}^{N_c} \ln [1 - 2\cos(\theta_i - \theta_j) e^{-\beta\epsilon_g(\vec{p})} + e^{-2\beta\epsilon_g(\vec{p})}] \right\} \\ & -(2J+1)(N_c-1)V \int \frac{d^3p}{(2\pi)^3} \ln [1 - e^{-\beta\epsilon_g(\vec{p})}]. \end{aligned} \quad (41)$$

Similar to the fundamental quark and antiquark canonical ensemble, the grand canonical ensemble for the adjoint gluons exhibits Gross-Witten Hagedorn transition. The grand canonical partition function above the point of the Gross-Witten Hagedorn transition can be approximated by the quadratic Taylor expansion around the saddle points as has been done for the quark and anti-quark grand canonical ensemble. The fact that the saddle points are convened at the origin simplifies the calculation remarkably. The quadratic Taylor expansion of the gluon grand canonical ensemble reads

$$\begin{aligned} \ln Z_g(\beta, V) = & a_g^{(0)} - \frac{1}{2}a_g \sum_{i=1}^{N_c} \sum_{j=1}^{N_c} (\theta_i - \theta_j)^2, \\ = & a_g^{(0)} - \frac{1}{2} \frac{(2N_c a_g^{(2)})}{2N_c} \sum_{i=1}^{N_c} \sum_{j=1}^{N_c} (\theta_i - \theta_j)^2, \end{aligned} \quad (42)$$



where

$$\begin{aligned}
a_g^{(0)} &= -(2J+1)V N_{adj} \int \frac{d^3 p}{(2\pi)^3} \ln(1 - e^{-\beta \epsilon_g(\vec{p})}), \\
&= (2J+1) \left( \frac{V}{\beta^3} \right) N_{adj} \left( \frac{\pi^2}{90} \right),
\end{aligned} \tag{43}$$

and

$$\begin{aligned}
a_g^{(2)} &= (2J+1)V \int \frac{d^3 p}{(2\pi)^3} \left[ \frac{e^{-\beta \epsilon_g(\vec{p})}}{1 - 2e^{-\beta \epsilon_g(\vec{p})} + e^{-2\beta \epsilon_g(\vec{p})}} \right], \\
&= (2J+1) \left( \frac{V}{\beta^3} \right) \left( \frac{1}{6} \right).
\end{aligned} \tag{44}$$

It should be noted that when the color-singlet state with the unimodular unitary symmetry group representation is projected by integrating the partition function over the invariance Haar measure  $\int d\mu Z_{q\bar{q}g}$  in the Hilbert space, the Fock space component of the adjoint gluon grand canonical ensemble is approximated to

$$\begin{aligned}
\ln Z_g(\beta, V) &= a_g^{(0)} - \frac{1}{2} \frac{(2N_c a_g^{(2)})}{2N_c} \sum_{i=1}^{N_c} \sum_{j=1}^{N_c} (\theta_i - \theta_j)^2, \\
&\equiv a_g^{(0)} - \frac{1}{2} (2N_c a_g^{(2)}) \sum_{i=1}^{N_c} \theta_i^2.
\end{aligned} \tag{45}$$

The second line in Eq.(45) is obtained under an appropriate transformation. The above procedure for calculating the canonical ensemble can be extrapolated to other symmetry groups such as the orthogonal and symplectic ones with the aim to avoid writing the adjoint representation for gluons explicitly. The same procedure still holds when an additional unimodular-like constraint is probed in the given symmetry group. This extrapolation is essential in order to simplify the calculation drastically. The grand canonical ensemble for a blob of quarks and gluons is the tensor product of the Fock spaces for the quark and anti-quark canonical partition function and the gluon canonical partition function. Therefore, the quark-gluon partition function just above the Gross-Witten Hagedorn transition from the discrete low-lying mass spectrum to the continuous high-lying mass spectrum reads

$$\begin{aligned}
Z_{q\bar{q}g}(\beta, V) &= \exp \left( a_{q\bar{q}}^{(0)} + a_g^{(0)} \right) e^{-\frac{1}{2} (a_{q\bar{q}}^{(2)} + 2N_c a_g^{(2)}) \sum_{i=1}^{N_c} \theta_i^2}, \\
&\equiv Z_{q\bar{q}g}(\theta_1, \dots, \theta_N).
\end{aligned} \tag{46}$$

The confined quark-gluon bag must be colorless. The color-singlet-state (colorless) bags correspond the Hagedorn states. The color-singlet grand canonical partition function for

the confined quark-gluon bag in the  $SU(N_c)$  representation reads

$$\begin{aligned}
Z_H(\beta, V) &= \int d\mu(g) Z_{q\bar{q}g}(\beta, V), \\
&\sim \frac{\exp(a_{q\bar{q}g}^{(0)})}{N_c!} \int \left( \prod_{n=1}^{N_c} \frac{d\theta_n}{2\pi} \right) 2\pi \delta \left( \sum_{i=1}^{N_c} \theta_i \right) \left( \prod_{j>i}^{N_c} (\theta_j - \theta_i)^2 \right) e^{-\frac{1}{2} a_{q\bar{q}g}^{(2)} \sum_i^{N_c} \theta_i^2}, \\
&\sim \frac{\exp(a_{q\bar{q}g}^{(0)})}{N_c!} \sqrt{\frac{2\pi a_{q\bar{q}g}^{(2)}}{N_c}} \int \left( \prod_{n=1}^{N_c} \frac{d\theta_n}{2\pi} \right) \left( \prod_{j>i}^{N_c} (\theta_j - \theta_i)^2 \right) e^{-\frac{1}{2} a_{q\bar{q}g}^{(2)} \sum_i^{N_c} \theta_i^2},
\end{aligned} \tag{47}$$

where

$$\begin{aligned}
a_{q\bar{q}g}^{(0)} &= a_{q\bar{q}}^{(0)} + a_g^{(0)}, \\
&= (2J+1) \left( \frac{V}{\beta^3} \right) \left( N_c \sum_{q=1}^{N_f} \left[ \frac{7\pi^2}{360} + \frac{1}{12} \left( \frac{\mu_q}{T} \right)^2 + \frac{1}{24\pi^2} \left( \frac{\mu_q}{T} \right)^4 \right] + N_{adj} \frac{\pi^2}{90} \right), \tag{48}
\end{aligned}$$

and

$$\begin{aligned}
a_{q\bar{q}g}^{(2)} &= a_{q\bar{q}}^{(2)} + 2N_c a_g^{(2)}, \\
&= (2J+1) \left( \frac{V}{\beta^3} \right) \left( \sum_{q=1}^{N_f} \frac{1}{6} \left[ 1 + \frac{3}{\pi^2} \left( \frac{\mu_q}{T} \right)^2 \right] + \frac{2N_c}{6} \right). \tag{49}
\end{aligned}$$

The partition function that is given by Eq.(47) leads to the high-lying continuous hadronic mass spectrum when it is transformed to the micro-canonical ensemble.

It is useful to mention the following relations. The canonical ensembles for adjoint particles in  $SU(N_c)$  and  $U(N_c)$  symmetry group representations are related by

$$\begin{aligned}
Z_{(Adj)} &= \int d\mu_{[U(N_c)]} e^{-\frac{1}{2} a_{Adj} \sum_i^{N_c} \sum_j^{N_c} (\theta_i^2 - \theta_j^2)^2}, \\
&\sim N_c \int d\mu_{[SU(N_c)]} e^{-\frac{1}{2} a_{Adj} \sum_i^{N_c} \sum_j^{N_c} (\theta_i^2 - \theta_j^2)^2}, \\
&\sim N_c \int d\mu_{[SU(N_c)]} e^{-\frac{1}{2} [2N_c a_{Adj}] \sum_i^{N_c} \theta_i^2}.
\end{aligned} \tag{50}$$

The canonical ensembles for gas of fundamental and adjoint particles in  $SU(N_c)$  and  $U(N_c)$  symmetry group representations are related in the following way:

$$\begin{aligned}
Z_{(Fun+Adj)} &= \int d\mu_{[U(N_c)]} e^{-\frac{1}{2} a_{Fun} \sum_i^{N_c} \theta_i^2 - \frac{1}{2} a_{Adj} \sum_i^{N_c} \sum_j^{N_c} (\theta_i^2 - \theta_j^2)^2}, \\
&\sim \frac{1}{\sqrt{a_{Fun}}} \int d\mu_{[SU(N_c)]} e^{-\frac{1}{2} a_{Fun} \sum_i^{N_c} \theta_i^2 - \frac{1}{2} a_{Adj} \sum_i^{N_c} \sum_j^{N_c} (\theta_i^2 - \theta_j^2)^2}, \\
&\sim \frac{1}{\sqrt{a_{Fun}}} \int d\mu_{[SU(N_c)]} e^{-\frac{1}{2} [a_{Fun} + 2N_c a_{Adj}] \sum_i^{N_c} \theta_i^2}.
\end{aligned} \tag{51}$$

### III. INTERNAL SYMMETRY

The canonical ensemble for the quark-gluon bag with specific internal symmetry is constructed in the standard way by defining the group's eigenvalues of the conserved color charges which are commutated with the Hamiltonian. The group's eigenvalues are defined by an appropriate transformation of the group's generators to take a diagonal format as follows

$$\sum_{i=1}^N a_i \mathbf{t}_i = \text{diag}(\theta_1, \dots, \theta_N), \quad (52)$$

where  $\mathbf{t}_i$  are the group's generators in the fundamental representation. The continuous group's parameters  $\theta_i$  (where  $i = 1, \dots, N$ ) are treated as variables of the conserved color charges which control the composite internal structure. In the same way, it is possible to write the diagonal form of the adjoint representation as follows

$$\sum_{a=1}^{N_{adj}} a_a \mathbf{T}_a = \text{diag}(\phi_1, \dots, \phi_{N_{adj}}). \quad (53)$$

The conserved charges in the adjoint representation depend essentially on the fundamental charges and they are written as functions of the fundamental charges:

$$\phi_a = f_a(\theta_1, \dots, \theta_N), \quad (54)$$

where the subscript index, namely,  $a$  runs over the adjoint index  $a = 1, \dots, N_{adj}$ . For instance with a suitable choice of the unitary representation  $U(N)$ , the conserved adjoint charges  $\phi_a$  are related to the fundamental charges  $\theta_i$  by  $\phi_{\underbrace{(ij)}} = (\theta_i - \theta_j)$ . The adjoint index  $a$  is written in term of the double fundamental indexes  $ij$ . The group's (energy-) eigenvalues which control the composite internal structure degrees of freedom correspond the conserved charges. The dual role of the group's energy-eigenvalues and the conserved charges is the mechanism behind the symmetry breaking/restoration (i.e. symmetry decomposition/reduction from symmetry group to another). It is responsible of the phase transition from a composite with a specific internal structure to another state with different symmetry configuration. This mechanism becomes obvious in the example of the phase transition scenario  $SU(N) \rightarrow U(1)^{N-1}$ . The chemical reaction fugacity and the set of characteristic chemical potentials of the conserved charges are realized by the analytic

continuation of the group eigenvalues  $i\theta_i \rightarrow -\beta\mu_i$ . The group invariance is transformed into system's fugacities  $\Lambda_i = e^{i\theta_i} \rightarrow \Lambda_i = e^{-\beta\mu_i}$ . The internal structure of the composite is incorporated by writing the canonical ensemble as a function of the group energy eigen-variables, namely,  $Z(\theta_1, \dots, \theta_N)$ . The easiest way to define the canonical ensemble of the composite in the Hilbert space is to write it as a tensor product of the Fock space canonical ensembles of the constituent quarks and gluons. The canonical ensemble for the quark-gluon bag is written as follows

$$\begin{aligned} Z_{q\bar{q}g}(\mathbf{R}(g)) &= \text{tr} [\mathbf{R}_{q\bar{q}g}(g) \exp(-\beta H_{q\bar{q}g})], \\ &= \text{tr} [\mathbf{R}_q(g) \exp(-\beta H_q)] \text{tr} [\mathbf{R}_{\bar{q}}(g) \exp(-\beta H_{\bar{q}})] \text{tr} [\mathbf{R}_g(g) \exp(-\beta H_g)]. \end{aligned} \quad (55)$$

The canonical ensemble for quark gas in the Fock space reads

$$\text{tr} [\mathbf{R}_q(g) \exp(-\beta H_q)] = \exp \left[ \sum_{\alpha} \text{tr} \ln (1 + \mathbf{R}_{fun}(g) e^{-\beta H_{q\alpha}}) \right], \quad (56)$$

while the canonical ensemble for gluon gas becomes

$$\text{tr} [\mathbf{R}_g(g) \exp(-\beta H_g)] = \exp \left[ - \sum_{\alpha} \text{tr} \ln (1 - \mathbf{R}_{adj}(g) e^{-\beta H_{g\alpha}}) \right]. \quad (57)$$

The internal structure is incorporated by the group eigenvalues of the conserved charges. The fundamental and adjoint color charges are specified, respectively, by

$$\mathbf{R}_{fun}(g) = U^{-1} (\exp [i \text{diag}(\theta_1, \dots, \theta_N)]) U, \quad (58)$$

and

$$\mathbf{R}_{adj}(g) = U_{adj}^{-1} (\exp [i \text{diag}(\phi_1, \dots, \phi_{N_{adj}})]) U_{adj}, \quad (59)$$

where  $U$  and  $U_{adj}$  are appropriate transformation matrices and they are reduced to the identity matrices (i.e.  $U = 1$  and  $U_{adj} = 1$ ) for the unitary group representation. Finally, the canonical ensemble with a specific internal structure is projected using the standard orthogonal expansion procedure. The specific symmetry state is projected by the integration of a specific projection state over the symmetry group invariance Haar measure in the following way,

$$Z_{\chi} = \int d\mu_G(\theta_1, \dots, \theta_N) [\chi \times Z(\theta_1, \dots, \theta_N)], \quad (60)$$

where  $\chi = \chi(\theta_1, \dots, \theta_N)$  is an orthogonal basis. The integral element  $d\mu_G$  is the symmetry group invariance Haar measure for a specific symmetry group. The invariance Haar measure is essential in order to accommodate the composite internal symmetry. The color confinement is manifested by maintaining the color singlet state. Fortunately, the singlet state is the simplest case and its basis is given by  $\chi_{singlet} = 1$ . The prime objective is to confine the quarks in a color singlet state regardless of the composite internal group symmetry.

### A. Unitary symmetry group $U(N)$

In the context of the unitary symmetry group transformation, the physical Hamiltonian is subject to the Hermitian condition

$$H = H^\dagger. \quad (61)$$

The unitary symmetry group subjects to the following constraint

$$U^\dagger U = 1, \text{ hence } U^{-1} = U^\dagger, \quad (62)$$

where the matrix  $U$  is a complex one and the Hermitian matrix is defined by  $U^\dagger = U^{*T}$ . The unitary matrix  $U$  has  $2N^2$  real parameters where  $N^2$  comes from the real part of the unitary matrix and  $N^2$  comes from the imaginary part. The unitary condition imposes  $[N + 2N(N - 1)/2]$  constraints on  $2N^2$  real parameters to give  $N_{adj} = N^2$  essential real parameters. Hence, the unitary symmetry has  $N_{fun} = N$  and  $N_{adj} = N^2$  for the fundamental and adjoint charges, respectively.

The Gaussian unitary ensemble multiplied by the group volume element is defined in terms of Hermitian matrices as follows

$$Z(H) dH \text{ (invariant) }, \quad (63)$$

which is invariant under automorphism unitary transformation. The invariance Haar measure is given by the volume element

$$dH = \prod_{k \leq j} dH_{jk}^{(0)} \prod_{k < j} dH_{kj}^{(1)}, \quad (64)$$

where  $H_{kj}^{(0)}$  and  $H_{kj}^{(1)}$  are real and imaginary parts of  $H_{kj}$ . The partition function  $Z(H)$  is a function of only the eigenvalues  $\theta_i$  where  $i$  runs over  $1, \dots, N$ . This means that the

Hermitian Hamiltonian commutes with the group generators those correspond the group eigenvalues  $\theta_i$  where  $i$  runs over  $1, \dots, N$ . The invariance Haar measure is reduced to

$$\begin{aligned} \int d\mu(\theta_1 \cdots \theta_N) &= N_U \frac{1}{N!} \int_{-\pi}^{\pi} \left( \prod_{i=1}^N \frac{d\theta_i}{2\pi} \right) \prod_{i<j}^N 4 (e^{i\theta_i} - e^{i\theta_j}) (e^{i\theta_i} - e^{i\theta_j})^* \\ &= N_U \frac{1}{N!} \int_{-\pi}^{\pi} \left( \prod_{i=1}^N \frac{d\theta_i}{2\pi} \right) \prod_{i<j}^N 4 \sin^2 \left( \frac{\theta_i - \theta_j}{2} \right), \end{aligned} \quad (65)$$

where  $-\pi \leq \theta_i \leq \pi$  for the circular ensemble. The variables  $(\theta_1, \dots, \theta_N)$  are the diagonalized group eigenvalues. The number of adjoint charges is reduced to  $N_{adj} = N^2$ . The normalisation constant  $N_U$  is determined by

$$\frac{1}{N_U} = \frac{1}{N!} \int_{-\pi}^{\pi} \left( \prod_{i=1}^N \frac{d\theta_i}{2\pi} \right) \prod_{i<j}^N 4 \sin^2 \left( \frac{\theta_i - \theta_j}{2} \right). \quad (66)$$

The saddle points of the group eigen-variables accumulate around the origin for the hot and dense nuclear matter under extreme conditions. Subsequently, the canonical ensemble can be written as the Gaussian-like ensemble in the following way,

$$\int d\mu(\theta_1 \cdots \theta_N) e^{-a \sum_i^N \theta_i^2}. \quad (67)$$

Therefore, the invariance Haar measure is approximated to

$$\begin{aligned} \int d\mu(\theta_1 \cdots \theta_N) (\cdots) &\approx N_U \frac{1}{N!} \int_{-\infty}^{\infty} \prod_{i=1}^N \frac{d\theta_i}{2\pi} \prod_{i<j}^N 4 \left( \frac{\theta_i - \theta_j}{2} \right)^2 (\cdots), \\ &\approx N_U \frac{1}{N!} \int_{-\infty}^{\infty} \prod_{i=1}^N \frac{d\theta_i}{2\pi} \prod_{i<j}^N (\theta_i - \theta_j)^2 (\cdots). \end{aligned} \quad (68)$$

The unimodular condition for the special unitary symmetry group  $SU(N)$  is imposed by

$$\sum_i^N \theta_i = 0. \quad (69)$$

Hence, the invariance Haar measure for  $SU(N)$  becomes

$$\begin{aligned} \int d\mu_{SU}(\theta_1 \cdots \theta_N) e^{-\frac{1}{2}a \sum_i^N \theta_i^2} &= N_U \frac{1}{N!} \int_{-\infty}^{\infty} \prod_{i=1}^N \frac{d\theta_i}{2\pi} 2\pi \delta \left( \sum_i^N \theta_i \right) \\ &\quad \times \prod_{i<j}^N (\theta_i - \theta_j)^2 e^{-\frac{1}{2}a \sum_i^N \theta_i^2}. \end{aligned} \quad (70)$$

By writing the delta function as

$$\delta\left(\sum_i^N \theta_i\right) = \int_{-\infty}^{\infty} dx \exp\left(i x \sum_i^N \theta_i\right), \quad (71)$$

the color-singlet state of the canonical ensemble for the unimodular-like  $U(N_c)$  (i.e.  $SU(N_c)$ ) reads

$$\int d\mu_{SU}(\theta_1 \cdots \theta_N) e^{-\frac{1}{2}a \sum_{i=1}^N \theta_i^2} = \sqrt{\frac{2\pi a}{N}} \int d\mu_U(\theta_1 \cdots \theta_N) e^{-\frac{1}{2}a \sum_{i=1}^N \theta_i^2}. \quad (72)$$

## B. Orthogonal symmetry group $O_{(S)}(N)$

The unitary Hermitian system may be decomposed into symmetric Hermitian and anti-symmetric Hermitian real orthogonal components. The orthogonal symmetry group is symmetric one and is invariant under the time-reversal transformation. The unitary Hermitian system can be fully or partially projected into (symmetric) orthogonal Hermitian system. The projection of the unitary Hermitian system into the real symmetric orthogonal system is very relevant to the quark-gluon plasma under extreme conditions such as the hot nuclear matter. The transformation matrix, namely,  $U$  of the orthogonal group is a symmetric one. It has  $N^2$  elements and these elements are restricted to  $N + N(N-1)/2$  conditions. These constraints reduce the number of the adjoint variables to  $N_{adj} = N(N-1)/2$  while the number of the fundamental variables remain the same  $N_{fun} = N$  in the orthogonal symmetry group. The invariance Haar measure for the orthogonal symmetry group reads

$$\int d\mu_{O(S)}(\theta_1 \cdots \theta_N) = N_O \int_{-\pi}^{\pi} \prod_{i=1}^N \frac{d\theta_i}{2\pi} \prod_{i<j}^N \left| \sin\left(\frac{\theta_i - \theta_j}{2}\right) \right|. \quad (73)$$

The normalisation constant  $N_U$  is determined by

$$N_O \int_{-\pi}^{\pi} \prod_{i=1}^N \frac{d\theta_i}{2\pi} \prod_{i<j}^N \left| 2 \sin\left(\frac{\theta_i - \theta_j}{2}\right) \right| = 1. \quad (74)$$

When the saddle points accumulate around the origin, the invariance Haar measure becomes

$$\int d\mu_{O(S)}(\theta_1 \cdots \theta_N) e^{-\frac{1}{2}a \sum_{i=1}^N \theta_i^2} = N_O \int_{-\infty}^{\infty} \prod_{i=1}^N \frac{d\theta_i}{2\pi} \prod_{i<j}^N |\theta_i - \theta_j| e^{-\frac{1}{2}a \sum_{i=1}^N \theta_i^2}. \quad (75)$$

The unimodular-like orthogonal  $O_{(S)}(N_c)$  symmetry group is constructed by imposing the unimodular-like constraint  $\sum_{i=1}^{N_c} \theta_i = 0$  to the standard orthogonal symmetry group. The color-singlet Gaussian integral for the unimodular-like orthogonal symmetry group  $SO_{(S)}(N)$  is related to  $O_{(S)}(N)$  in the following way

$$\begin{aligned} & \int d\mu_{O_{(S)}}(\theta_1 \cdots \theta_N) e^{-\frac{1}{2}a \sum_{i=1}^N \theta_i^2}, \quad (\text{with the unimodular-like constraint}), \\ & \sim \int d\mu_{O_{(S)}}(\theta_1 \cdots \theta_N) 2\pi \delta\left(\sum_{i=1}^N \theta_i\right) e^{-\frac{1}{2}a \sum_{i=1}^N \theta_i^2} \\ & \sim \sqrt{\frac{2\pi a}{N}} \int d\mu_{O_{(S)}}(\theta_1 \cdots \theta_N) e^{-\frac{1}{2}a \sum_{i=1}^N \theta_i^2}. \end{aligned} \quad (76)$$

### C. Symplectic symmetry group $Sp(N)$ ( $N$ is the number of quaternion)

The symplectic symmetry group is time-reversal invariance. The anti-symmetrization in the symmetry group  $Sp(N)$  leads to odd-spin. The algebra of the symplectic symmetry group can be expressed in terms of quaternions. The quaternions are convenient to deal with the anti-symmetrization. The notation  $Sp(N)$  is equivalent to  $Sp(2N, R)$  where  $N$  corresponds to the number of quaternions.

The transformation matrix  $U$  of the  $Sp(N)$  group is of the size of  $(2N \times 2N)$ . This transformation matrix is considered as cut into  $N^2$  blocks of  $2 \times 2$  and each  $2 \times 2$  block is expressed in terms of the quaternions. In this sense the number of real independent parameters these are defined in the  $(2N \times 2N)$  self-dual Hermitian matrix is given by the number of the adjoint variables  $N_{adj}$ . The number of the fundamental (energy-) eigen variables is  $N_{fun} = N$  while the number of the adjoint variables is  $N_{adj} = N(2N - 1)$ . The invariance Haar measure for the symplectic symmetry group  $Sp(N)$  with the circular canonical ensemble is given by

$$\int d\mu_{Sp}(\theta_1 \cdots \theta_N) = N_{Sp} \int_{-\pi}^{\pi} \prod_{i=1}^N \frac{d\theta_i}{2\pi} \prod_{i < j} \left[ 4 (e^{i\theta_i} - e^{i\theta_j}) (e^{i\theta_i} - e^{i\theta_j})^* \right]^2. \quad (77)$$

The normalisation constant  $N_{Sp}$  is determined by

$$\frac{1}{N_{Sp}} = \int_{-\pi}^{\pi} \prod_{i=1}^N \frac{d\theta_i}{2\pi} \prod_{i < j} 16 \sin^4 \left( \frac{\theta_i - \theta_j}{2} \right). \quad (78)$$

Under extreme conditions, the saddle points of the group continuous variables accumulate around the origin. Therefore, the canonical ensemble is approximated to the Gaussian-like



ensemble in the following way

$$\int d\mu_{Sp}(\theta_1 \cdots \theta_N) e^{-a \sum_i^{N_c} \theta_i^2 + b \sum_i^{N_c} \theta_i + c}, \quad (79)$$

where  $a$  is real and positive and  $b$  and  $c$  are real. The invariance Haar measure for  $Sp(N)$  is approximated to

$$\int d\mu_{Sp}(\theta_1 \cdots \theta_N)(Z) \approx N_{Sp} \int_{-\infty}^{\infty} \prod_{i=1}^N \frac{d\theta_i}{2\pi} \prod_{i<j}^N (\theta_i - \theta_j)^4(Z). \quad (80)$$

The result for the canonical partition function with the symplectic symmetry group can be extrapolated around the saddle points to take the following general formula

$$\begin{aligned} Z(\text{I.S.}) &= \int_{-\pi}^{\pi} d\mu_{Sp}(\theta_1, \theta_2, \cdots, \theta_N) Z(\theta_1, \theta_2, \cdots, \theta_N), \\ &= Z_0 \int_{-\infty}^{\infty} d\mu_{Sp}(\theta_1, \theta_2, \cdots, \theta_N) e^{-\frac{1}{2}a \sum_{i=1}^N \theta_i^2}, \end{aligned} \quad (81)$$

where  $Z(\theta_1, \theta_2, \cdots, \theta_N) \approx Z_0(\{\theta_i \approx 0\}) e^{-\frac{1}{2}a \sum_{i=1}^N \theta_i^2}$ . The abbreviation (I.S.) means that the internal structure and the group variables satisfy the constraint  $(\theta_1 - \pi) \leq \theta_2 \leq \cdots \leq \theta_{2N} \leq (\theta_1 + \pi)$ . When the unimodular-like constraint is imposed (i.e.  $\sum_i^N \theta_i = 0$ ), the color-singlet state of the (unimodular-like) symplectic canonical ensemble is reduced to

$$Z(\text{I.S.}) \sim Z_0 \times N_{Sp} \sqrt{\frac{2\pi a}{N}} \int_{-\infty}^{\infty} \prod_{i=1}^N \frac{d\theta_i}{2\pi} \prod_{i<j}^N (\theta_i - \theta_j)^4 \left( e^{-\frac{1}{2}a \sum_{i=1}^N \theta_i^2} \right). \quad (82)$$

#### IV. EQUATION OF STATE FOR COMPOSITE NUCLEAR MATTER

The color-singlet-state unitary (mixed-grand) canonical ensemble can be extrapolated to another color-singlet-state ensemble with different symmetry groups. The most important issue in the extrapolation from one symmetry group to another one is that these symmetry groups have the same number  $N_c$  of fundamental Fourier color charges (i.e. group eigenvariables). The difference among various symmetry groups comes from the difference in the numbers of the conserved adjoint Fourier charges with the same number of fundamental Fourier charges. The second difference comes from the different invariance Haar measure for every kind of symmetry group. The invariance Haar measure for each symmetry group is essential in order to project the color-singlet-state of the quark and gluon bag. Therefore, the effective Vandermonde potential is modified drastically when the internal symmetry is transferred from one symmetry group to another one.

The canonical ensemble with specific internal symmetry group and that is projected to a certain quantum wavefunction is given by

$$\begin{aligned} Z_{state}(\beta, V) &= \int d\mu_G(g) [\chi_{state} \times Z_{q\bar{q}g}(\beta, V; \theta_1, \dots, \theta_N)], \\ &\sim \mathcal{N} Z_0(\beta, V) \int \left( \prod_{n=1}^{N_c} d\theta_n \right) \prod_{j>i} |\theta_j - \theta_i|^G (\chi_{state}) e^{-\frac{1}{2} a_{q\bar{q}g}^{(2)} \sum_i^{N_c} \theta_i^2}, \end{aligned} \quad (83)$$

where  $Z_0(\beta, V) = \exp(a_{q\bar{q}g}^{(0)})$ . The symmetry group structure is defined by  $G = 1, 2, 4$  for the orthogonal, unitary and symplectic ensemble, respectively. The color-singlet-state quantum wave-function is given by  $\chi_{singlet} = 1$  regardless of the symmetry group. In general the physical state in QCD is assumed to satisfy the condition  $\det(G) = 1$  or equivalently it is restricted to the unimodular-like constraint, namely,  $\sum_{i=1}^{N_c} \theta_i = 0$ . The unimodular-like constraint modifies the extrapolated color-singlet-state canonical Gaussian ensemble with a specific group such as unitary, orthogonal and symplectic symmetry groups to the following quantity

$$\begin{aligned} Z_{singlet}(\beta, V) &\sim \mathcal{N} Z_0(\beta, V) \sqrt{\frac{2\pi a_{q\bar{q}g}^{(2)}}{N_c}} \int \left( \prod_{n=1}^{N_c} d\theta_n \right) \prod_{j>i} |\theta_j - \theta_i|^G \\ &\times e^{-\frac{1}{2} a_{q\bar{q}g}^{(2)} \sum_{i=1}^{N_c} \theta_i^2}, \end{aligned} \quad (84)$$

where  $\mathcal{N} = N_U, N_O$  and  $N_{Sp}$  for the unitary, orthogonal and symplectic symmetry groups, respectively. Eq.(84) is derived by imposing the unimodular-like constraint using the following trick

$$\delta \left( \sum_{i=1}^N \theta_i \right) = \int_{-\infty}^{\infty} dx e^{ix \sum_1^N \theta_i}. \quad (85)$$

The integral part in Eq.(84) is evaluated as follows

$$\begin{aligned} I &= \int \left( \prod_{n=1}^{N_c} d\theta_n \right) \prod_{j>i} |\theta_j - \theta_i|^G e^{-\frac{1}{2} a_{q\bar{q}g}^{(2)} \sum_{i=1}^{N_c} \theta_i^2}, \\ &= \left( \frac{G}{a_{q\bar{q}g}^{(2)}} \right)^{G(N_c^2 - N_c)/4 + N_c/2} \int_{-\infty}^{\infty} \left( \prod_{n=1}^{N_c} dx_n \right) \prod_{j>i} |x_j - x_i|^G e^{-\frac{1}{2} G \sum_i^{N_c} x_i^2}, \\ &= \mathcal{N}_{N_c G} \left( \frac{G}{a_{q\bar{q}g}^{(2)}} \right)^\alpha. \end{aligned} \quad (86)$$

The exponent  $\alpha$  is determined by

$$\alpha = G(N_c^2 - N_c)/4 + N_c/2. \quad (87)$$

In QCD where the number of colors becomes  $N_c = 3$ , the exponent  $\alpha$  is reduced to 3, 9/2 and 15/2 for the orthogonal, unitary and symplectic color-singlet ensembles, respectively, and these groups are fallen under an additional unimodular-like constraint. The normalisation constant is determined by

$$\mathcal{N}_{N_c G} = (2\pi)^{\frac{N_c}{2}} G^{-\alpha} \prod_{n=1}^{N_c} \Gamma\left(1 + \frac{1}{2} G n\right) / \left[\Gamma\left(1 + \frac{1}{2} G\right)\right]^{N_c}, \quad (88)$$

where  $G = 1, 2$  and  $4$  for the orthogonal, unitary and symplectic symmetry groups, respectively. It should be noted that  $\Gamma(n)$  is the gamma function. The color-singlet-state canonical ensemble with a certain internal symmetry that is fallen under the additional unimodular-like condition is reduced to the following general formula,

$$Z_{singlet}(\beta, V) \sim \sqrt{2\pi/N_c} \mathcal{N} \mathcal{N}_{N_c G} G^\alpha \left(a_{q\bar{q}g}^{(2)}\right)^{-(\alpha-1/2)} \exp\left(a_{q\bar{q}g}^{(0)}\right). \quad (89)$$

When the term  $(V/\beta^3)$  is parameterised, the color-singlet-state (mixed-grand) canonical ensemble which is given in Eq.(89) becomes

$$Z_{q\bar{q}g}(\beta, V) = C_{N_c G} \left(\frac{\beta^3/V}{\tilde{a}_{q\bar{q}g}^{(2)}}\right)^{\alpha-\frac{1}{2}} \exp\left(\frac{V}{\beta^3} \tilde{a}_{q\bar{q}g}^{(0)}\right). \quad (90)$$

where

$$\begin{aligned} \tilde{a}_{q\bar{q}g}^{(0)} &= a_{q\bar{q}g}^{(0)} / \left(\frac{V}{\beta^3}\right), \\ \tilde{a}_{q\bar{q}g}^{(2)} &= a_{q\bar{q}g}^{(2)} / \left(\frac{V}{\beta^3}\right). \end{aligned} \quad (91)$$

The normalisation constant  $C_{N_c G}$  for short reads

$$C_{N_c G} = \sqrt{2\pi/N_c} \mathcal{N} \mathcal{N}_{N_c G} G^\alpha. \quad (92)$$

We can relax the definition of the normalisation constant, namely,  $C_{N_c G}$ . This modified constant  $C_{N_c G}$  will be determined from the physical constraint in order to satisfy the thermodynamic ensemble under realistic situations. The thermodynamic ensemble is concave up with respect to the variable  $x = V/\beta^3$  [1]. It is evident that the physical threshold must start from bottom point of the concave up curve. The line on the left hand side of the threshold point is unphysical and must be excluded. This behaviour furnishes an additional physical constraint that mentioned above. This provides a strong signature that analytical solution has been changed somewhere on the right hand side of the threshold point. The change in

the analytical solution behaviour indicates that the canonical ensemble transmutes from one state to another but the deconfinement phase transition is still not reached yet. Furthermore, the value of the thermodynamic ensemble above the threshold of the Gross-Witten point is restricted to fall in a physical region (i.e. non-negative) as follows,

$$\ln [Z_{q\bar{q}g}(\text{threshold})] \geq 0. \quad (93)$$

The critical (threshold) point  $x_c \equiv x_{min}$  is calculated by extremizing the logarithm of the canonical ensemble. The canonical ensemble is written as follows

$$\begin{aligned} Z_{q\bar{q}g}(x) &\sim C \left( \tilde{a}_{q\bar{q}g}^{(2)} x \right)^{-(\alpha-1/2)} \exp \left( \tilde{a}_{q\bar{q}g}^{(0)} x \right), \\ \ln Z_{q\bar{q}g}(x) &\sim -(\alpha - 1/2) \ln(x) + \tilde{a}_{q\bar{q}g}^{(0)} x + \left[ \ln C - (\alpha - 1/2) \ln \tilde{a}_{q\bar{q}g}^{(2)} \right]. \end{aligned} \quad (94)$$

The value of the relaxation constant  $C = C_{N_c G}$  is fixed in order to regulate the solution and match some physical requirements [1]. The threshold point  $x_{th}$  is determined by calculating the minimum point of the concave up curve as follows

$$\begin{aligned} x_{th} &= x_{min}, \\ &= (\alpha - 1/2) / \tilde{a}_{q\bar{q}g}^{(0)}. \end{aligned} \quad (95)$$

The limit of the normalisation constant  $C$  is determined by

$$\ln Z(x_{th}) \geq \ln Z_0 \geq 0. \quad (96)$$

The energy threshold is found

$$\begin{aligned} \left( \frac{V}{\beta^3} \right) \Big|_{th} &= x_{th}, \\ &= (\alpha - 1/2) / \tilde{a}_{q\bar{q}g}^{(0)}. \end{aligned} \quad (97)$$

The threshold Hagedorn mass is estimated from  $\left( \frac{V}{\beta^3} \right) \Big|_{threshold}$ . As it will be demonstrated below when the canonical ensemble is transformed to the micro-canonical ensemble using Eq.(101), the saddle point method leads to the following dual connection

$$\left( \frac{V}{\beta^3} \right) \rightarrow \frac{1}{3\tilde{a}_{q\bar{q}g}^{(0)}} \left( 3\tilde{a}_{q\bar{q}g}^{(0)} V W^3 \right)^{1/4}. \quad (98)$$

In the context of standard MIT bag model, the above relation is reduced to

$$\begin{aligned} \left( \frac{V}{\beta^3} \right) &\rightarrow \frac{m}{4 (\tilde{a}_{q\bar{q}g}^{(0)})^{3/4} B^{1/4}}, \\ &\geq \left( \alpha - \frac{1}{2} \right) \left( \frac{1}{\tilde{a}_{q\bar{q}g}^{(0)}} \right), \end{aligned} \quad (99)$$

where  $B$  is the MIT bag constant. The bag constant is assigned to be approximately  $B^{1/4} \approx 200$  MeV. The constraint of Hagedorn mass threshold becomes

$$m_{threshold} \geq 4 \left( \alpha - \frac{1}{2} \right) \left( \frac{B}{\tilde{a}_{q\bar{q}g}^{(0)}} \right)^{1/4}. \quad (100)$$

The asymptotic density of states for the micro-canonical ensemble with large blob energy  $W$  is calculated by taking the inverse Laplace transform for the grand canonical ensemble. The inverse Laplace transform for large  $W$  is evaluated using the steepest descent method,

$$\begin{aligned} Z_{q\bar{q}g}(W, V) &= \frac{1}{2\pi i} \int_{\beta_0 - i\infty}^{\beta_0 + i\infty} d\beta e^{\beta W} Z_{q\bar{q}g}(\beta, V) \\ &= \frac{1}{2\pi i} \int_{\beta_0 - i\infty}^{\beta_0 + i\infty} d\beta \left[ C \left( \tilde{a}_{q\bar{q}g}^{(2)} \frac{V}{\beta^3} \right)^{-\alpha + \frac{1}{2}} e^{\beta W + \frac{V}{\beta^3} \tilde{a}_{q\bar{q}g}^{(0)}} \right]. \end{aligned} \quad (101)$$

The straightforward calculation leads to the following micro-canonical ensemble,

$$Z_{q\bar{q}g}(W, V) = C^* \frac{1}{W} \left[ \left( 3\tilde{a}_{q\bar{q}g}^{(0)} V W^3 \right)^{1/4} \right]^{-(\alpha-1)} \exp \left[ \frac{4}{3} \left( 3\tilde{a}_{q\bar{q}g}^{(0)} V W^3 \right)^{1/4} \right], \quad (102)$$

where

$$C^* = \frac{1}{2\sqrt{2\pi}} C \left( \frac{3\tilde{a}_{q\bar{q}g}^{(0)}}{\tilde{a}_{q\bar{q}g}^{(2)}} \right)^{\alpha-1/2}. \quad (103)$$

The saddle point of the Laplace transform is found

$$\beta = \frac{1}{W} \left[ 3\tilde{a}_{q\bar{q}g}^{(0)} V W^3 \right]^{1/4}. \quad (104)$$

In the standard MIT bag model, the bag's mass and volume are given by the following relations

$$\begin{aligned} m &= W + BV, \\ m &= 4BV, \\ W &= \frac{3}{4}m, \\ V &= \frac{m}{4B}, \\ \left( 3\tilde{a}_{q\bar{q}g}^{(0)} V W^3 \right)^{1/4} &= \frac{3}{4} \left( \frac{\tilde{a}_{q\bar{q}g}^{(0)}}{B} \right)^{1/4} m. \end{aligned} \quad (105)$$

The density of states for the continuous high-lying mass spectrum is given by calculating the canonical ensemble and its transformation to the micro-canonical ensemble. The continuous high-lying mass spectral densities for the color-singlet-state orthogonal, unitary and

symplectic symmetry groups with an additional unimodular-like constraint are reduced to the following general form

$$\rho_{high}(m) = \frac{4}{3} C^* \left[ \frac{3}{4} \left( \frac{\tilde{a}_{q\bar{q}g}^{(0)}}{B} \right)^{1/4} \right]^{-\alpha+1} m^{-\alpha} \exp \left[ \left( \frac{\tilde{a}_{q\bar{q}g}^{(0)}}{B} \right)^{1/4} m \right]. \quad (106)$$

The value of the exponent  $\alpha = G(N_c^2 - N_c)/4 + N_c/2$  depends on the bag's internal symmetry and again  $G = 1, 2$  and  $4$  correspond the orthogonal, unitary and symplectic symmetry groups, respectively. The unimodular-like constraint is assumed implicitly in all symmetry groups those are considered in the present work. The normalisation constant  $C^*$  depends on the group kind. Moreover, the continuous high-lying mass spectral density is simplified to

$$\left. \begin{aligned} \rho_{II}(m) &= \rho_{high}(m), \\ \rho_{high}(m) &= c m^{-\alpha} e^{bm}, \\ b &= \left( \frac{\tilde{a}_{q\bar{q}g}^{(0)}}{B} \right)^{1/4}, \\ c &\sim \frac{4}{3} C^* \left[ \frac{3}{4} \left( \frac{\tilde{a}_{q\bar{q}g}^{(0)}}{B} \right)^{1/4} \right]^{-\alpha+1} \end{aligned} \right\}. \quad (107)$$

The mass spectral exponent  $\alpha$  in the mass spectral density  $\rho_{II}(m)$  is reduced to  $\alpha = \frac{N_c^2}{4} + \frac{N_c}{4}$ ,  $\alpha = \frac{N_c^2}{2}$  and  $\alpha = N_c^2 - \frac{N_c}{2}$  for the unimodular-like orthogonal, unitary and symplectic Hagedorn states, respectively. Furthermore, the density of states for the colored bags with color  $SU(N_c)$  symmetry group (i.e. non-singlet color states) can be written in similar manner but the mass spectral exponent  $\alpha$  takes the minimum value  $\alpha = \frac{1}{2}$  regardless the number of colors.

The scenario of the phase transition for the dilute and hot nuclear matter (i.e.  $\mu_B \approx 0$  and  $T \rightarrow T_{critical}$ ) seems to pass multi-process phase transitions. The color-singlet-state  $SU(N_c)$  symmetry group (Hagedorn states) is broken to the color-singlet-state unimodular-like  $U(1)^{N_c}$  symmetry group (equivalent to  $U(1)^{N_c-1}$ ) and, subsequently, the number of adjoint color degrees of freedom is reduced from  $N_c^2 - 1$  to  $N_c - 1$ . This can be interpreted that  $N_c^2 - N_c$  gluon degrees of freedom are released from the unitary Hagedorn states when they are mutated to  $U(1)^{N_c}$  Hagedorn states. Furthermore, the symmetry transmutation from the  $SU(N_c)$  color-singlet state to the  $U(1)^{N_c}$  color-singlet state likely takes place through the intermediate the  $O_S(N_c)$  color-singlet state.

The crucial phenomenon of the model is that the quarks and anti-quarks tends to be confined in the  $U(1)^{N_c}$  Hagedorn states (i.e. colorless states). These states can be interpreted as quark liquid bubbles. The construction of the color-singlet-state for (unimodular-like)  $U(1)^{N_c}$  quark-bag is different from those for the color-singlet-state bags with the unitary, orthogonal and symplectic internal symmetry groups with the unimodular-like constraint. The  $U(1)^{N_c}$  symmetry group maintains the minimal gluonic content in the quark-bag (i.e. the minimal interaction among the quarks and antiquarks since  $N_{fun} = N_c$  and  $N_{adj} = N_c$ ). The  $U(1)^{N_c}$  color-singlet-state canonical ensemble for quark and antiquark bag is constructed in the following way

$$\begin{aligned} Z_{qbag}(\beta, V) &= \left[ \int d\mu_{U(1)}(\theta) Z_{q\bar{q}g}(\beta, V, \theta) \right]^{N_c-1}, \\ &= \left[ \frac{1}{2\pi} \int_{-\pi}^{\pi} d\theta Z_{q\bar{q}g}(\beta, V; \theta) \right]^{N_c-1}. \end{aligned} \quad (108)$$

Instead of considering the  $U(1)^{N_c}$  symmetry group, the  $U(1)^{N_c}$  symmetry group with the unimodular-like constraint  $\left(\sum_i^{N_c} \theta_i = 0\right)$  is adopted in order to be consistent with unitary, orthogonal and symplectic symmetry groups those are restricted to the unimodular-like condition and have the same number of the fundamental color charges. Hence, the canonical ensemble for the  $U(1)^{N_c}$  color-singlet state of the quark-bag is constructed as follows

$$\begin{aligned} Z_{qbag}(\beta, V) &= \int \prod_i d\mu_{U(1)}(\theta_i) 2\pi\delta\left(\sum_i^{N_c} \theta_i\right) \prod_i^{N_c} Z_{q\bar{q}g}(\beta, V, \theta_i), \\ &= \int \prod_i^{N_c} \frac{d\theta_i}{2\pi} 2\pi\delta\left(\sum_j^{N_c} \theta_j\right) \prod_k^{N_c} Z_{q\bar{q}g}(\beta, V, \theta_k), \end{aligned} \quad (109)$$

where it is restricted to the unimodular-like constraint. At extreme condition, it is reduced to

$$\begin{aligned} Z_{qbag}(\beta, V) &= \sqrt{\frac{2\pi}{N_c} \frac{V}{\beta^3} \tilde{u}_{q\bar{q}g}^{(2)}} \exp\left(\frac{V}{\beta^3} \tilde{u}_{q\bar{q}g}^{(0)}\right) \int \prod_i^{N_c} \frac{d\theta_i}{2\pi} \exp\left(-\frac{1}{2} \frac{V}{\beta^3} \tilde{u}_{q\bar{q}g}^{(2)} \sum_i^{N_c} \theta_i^2\right), \\ &= \frac{1}{\sqrt{N_c}} (2\pi)^{-N_c/2+1/2} \left(\frac{V}{\beta^3} \tilde{u}_{q\bar{q}g}^{(2)}\right)^{-N_c/2+1/2} \exp\left(\frac{V}{\beta^3} \tilde{u}_{q\bar{q}g}^{(0)}\right), \end{aligned} \quad (110)$$

where

$$\begin{aligned} \tilde{u}_{q\bar{q}g}^{(0)} &= (2J+1)N_c \sum_{f=1}^{N_f} \left[ \frac{7\pi^2}{360} + \frac{1}{12} \left(\frac{\mu_f}{T}\right)^2 + \frac{1}{24\pi^2} \left(\frac{\mu_f}{T}\right)^4 \right] \\ &\quad + (2J+1)N_c \left(\frac{\pi^2}{90}\right), \end{aligned} \quad (111)$$

and

$$\tilde{u}_{q\bar{q}g}^{(2)} = (2J+1) \sum_{f=1}^{N_f} \frac{1}{6} \left[ 1 + \frac{3}{\pi^2} \left( \frac{\mu_f}{T} \right)^2 \right] + (2J+1) \left( \frac{1}{6} \right). \quad (112)$$

The color-singlet-state micro-canonical ensemble for the unimodular-like  $U(1)^{N_c}$  symmetry reads

$$Z_{qbag}(W, V) = C_{qb} \frac{1}{W} \left[ \left( 3\tilde{u}_{q\bar{q}g}^{(0)} V W^3 \right)^{1/4} \right]^{-(\frac{N_c}{2}-1)} \exp \left[ \frac{4}{3} \left( 3\tilde{u}_{q\bar{q}g}^{(0)} V W^3 \right)^{\frac{1}{4}} \right], \quad (113)$$

where

$$C_{qb} = \frac{1}{2\sqrt{N_c}} (2\pi)^{-N_c/2} \left( \frac{3\tilde{u}_{q\bar{q}g}^{(0)}}{\tilde{u}_{q\bar{q}g}^{(2)}} \right)^{\frac{N_c}{2}-\frac{1}{2}}. \quad (114)$$

Furthermore, using the standard MIT bag model approximation, the mass spectral density is reduced to

$$\begin{aligned} \rho_{(II)} &= \rho_{qbag}(m), \\ &= \frac{4}{3} C_{qb} \left[ \frac{3}{4} \left( \frac{\tilde{u}_{q\bar{q}g}^{(0)}}{B} \right)^{\frac{1}{4}} \right]^{-\frac{N_c}{2}+1} m^{-\frac{N_c}{2}} \exp \left[ \left( \frac{\tilde{u}_{q\bar{q}g}^{(0)}}{B} \right)^{\frac{1}{4}} m \right]. \end{aligned} \quad (115)$$

The high-lying mass spectral density for the color-singlet-state (unimodular-like)  $U(1)^{N_c}$  symmetry quark-bag reads,

$$\begin{aligned} \rho_{(II)}(m) &= \rho_{qbag}(m), \\ &= c_{qb} m^{-\alpha_{qb}} e^{b_{qb} m}, \\ &\equiv c m^{-\alpha} e^{b m}, \end{aligned} \quad (116)$$

where  $\alpha = \alpha_{qb} = N_c/2$  and

$$\begin{aligned} c_{qb} &= \frac{4}{3} C_{qb} \left[ \frac{3}{4} \left( \frac{\tilde{u}_{q\bar{q}g}^{(0)}}{B} \right)^{\frac{1}{4}} \right]^{-\frac{N_c}{2}+1}, \\ b_{qb} &= \left( \frac{\tilde{u}_{q\bar{q}g}^{(0)}}{B} \right)^{\frac{1}{4}}. \end{aligned} \quad (117)$$

Generally speaking, it is possible to write the high lying mass spectral density as a linear combination of the Hagedorn states with different internal symmetries in the following way,

$$\rho_{(II)}(m) = \sum_i^{\text{symmetries}} a_{(i)} \rho_{(II)}^{(i)}(m), \quad (118)$$



where the index  $i$  run over the unimodular-like orthogonal  $O_S(N_c)$ , unitary  $U(N_c)$ , symplectic  $Sp(N_c)$  and  $U(1)^{N_c}$  Hagedorn states, respectively.

The hadronic matter consists all the known discrete low-lying mass spectrum particles those are found in the data book [3] and the continuous high-lying mass spectrum for the Hagedorn states with various internal structures. For instance the the data book [3] consists of 76 non-strange mesons and 64 non-strange baryons besides strange and other flavor hadrons. The density of states can be written as follows

$$\rho(T, \Lambda, m) = \rho_{(I)}(T, \Lambda, m) + \rho_{(II)}(T, \Lambda, m). \quad (119)$$

The first term on the right hand side of Eq.(119) is the discrete low-lying hadron mass spectrum

$$\begin{aligned} \rho_{(I)}(T, \Lambda, m) = & \sum_M^{mesons} \delta(m - m_M) \delta(\Lambda - \Lambda_M) + \sum_B^{baryons} \delta(m - m_B) \delta(\Lambda - \Lambda_B) \\ & + \sum_E^{exotic} \delta(m - m_E) \delta(\Lambda - \Lambda_E) \end{aligned} \quad (120)$$

where  $m_M$  and  $\Lambda_M$ , respectively, are the meson's mass and fugacity and  $m_B$  and  $\Lambda_B$ , respectively, are the baryon's mass and fugacity while  $m_E$  and  $\Lambda_E$ , respectively, are exotic particle's mass and fugacity. The baryon and meson mass spectra are satisfying the Fermi-Dirac and Bose-Einstein statistics, respectively. The exotic particle satisfies either Fermi-Dirac or Bose-Einstein statistics depends on the number of its constituent quarks and antiquarks. Since the discrete low-lying mass spectrum is limited for a relatively light hadron mass  $m \leq m_{critical} \approx 2$  GeV for non-strange hadrons, the Fermi-Dirac and Bose-Einstein are distinctive and they are taken exactly:

$$\begin{aligned} I = & Z_{(I)}(T, V; \Lambda), \\ = & \exp \left( \int_0^{m_0} dm \rho_{(I)}(T, \Lambda, m) [\ln z_{(Stats)}(T, m, \Lambda) + \ln z_{(Stats)}(T, m, \Lambda^{-1})] \right), \\ = & Z_{(I)}(T, V; \Lambda, \text{Mesons}) \times Z_{(I)}(T, V; \Lambda, \text{Baryons}) \\ & \times Z_{(I)}(T, V; \Lambda, \text{Exotics}), \end{aligned} \quad (121)$$

where the subscript notation, namely,  $(Stats)$  indicates either Fermi-Dirac or Bose-Einstein statistics for baryons or mesons, respectively. The low-lying mass spectrum ensemble is

decomposed into mesonic, baryonic and exotic ensembles as follows

$$Z_{(I)}(T, V; \Lambda, \text{Mesons}) = \prod_M^{\text{Mesons}} [z_{BE}(T, m_M, \Lambda_M) \times z_{BE}(T, m_M, \Lambda_M^{-1})], \quad (122)$$

and

$$Z_{(I)}(T, V; \Lambda, \text{Baryons}) = \prod_B^{\text{Baryons}} [z_{FD}(T, m_B, \Lambda_B) \times z_{FD}(T, m_B, \Lambda_B^{-1})], \quad (123)$$

as well as

$$\begin{aligned} Z_{(I)}(T, V; \Lambda, \text{Exotics}) &= \prod_E^{\text{Exotics}} [z_{BE}(T, m_E, \Lambda_E) \times z_{BE}(T, m_E, \Lambda_E^{-1})] \\ &\times \prod_E^{\text{Exotics}} [z_{FD}(T, m_E, \Lambda_E) \times z_{FD}(T, m_E, \Lambda_E^{-1})], \\ &\approx \exp[\text{negligible}] \approx 1. \end{aligned} \quad (124)$$

The exotic hadrons are suppressed because of their relative large masses in comparison to the ordinary mesons and baryons. Hence its contribution to the discrete hadronic mass spectrum is negligible.

The Fermi-Dirac and Bose-Einstein statistics, respectively, read

$$z_{FD}(T, m, \Lambda_B) = \exp \left[ (2J_B + 1)V \int \frac{d^3k}{(2\pi)^3} \ln \left( 1 + \Lambda_B e^{-\sqrt{(k^2 + m_B^2)}/T} \right) \right], \quad (125)$$

and

$$z_{BE}(T, m, \Lambda_M) = \exp \left[ -(2J_M + 1)V \int \frac{d^3k}{(2\pi)^3} \ln \left( 1 - \Lambda_M e^{-\sqrt{(k^2 + m_M^2)}/T} \right) \right]. \quad (126)$$

The mesonic and baryonic fugacities are given by  $\Lambda_M = e^{(S\mu_S)/T}$  and  $\Lambda_B = e^{(\mu_B + S\mu_S)/T}$ , respectively, where  $S = 0, -1$  etc is the strangeness quantum number.

The second term  $\rho_{(II)}(T, \Lambda, m)$  on the right hand side of Eq.(119) is the continuous high-lying mass spectrum and corresponds the Hagedorn's density of states. These states correspond the hadronic bubbles with relatively large hadronic masses and they appear as fireballs just above the highest known hadronic particles those are represented by the discrete low-lying mass spectrum. The Hagedorn threshold is estimated to be  $m \geq 2$  GeV for the non-strange hadrons. In the simplest approximation, the mass of the composite hadron is considered relatively large and the flavor degree of freedom is assumed to maintain the maximal invariance. Such exotic hadrons (Hagedorns) have no reason to prefer

the Fermi-Dirac or Bose-Einstein Statistics. These Hagedorn states are assumed to obey the classical Maxwell-Boltzmann statistics for the simplicity due to their relatively large masses. Nonetheless, in any realistic physical situation, the Hagedorn states violate the flavor invariance and this violation becomes negligible when the medium tends to be extreme hot and the chiral symmetry tends to be restored (i.e. there is no sufficient time for the flavor violation). Furthermore, the Maxwell-Boltzmann statistics is not adequate one for the highly compressed cold (or slight warm  $T \approx \text{few tens MeV}$ ) nuclear matter. In the case of highly compressed nuclear matter where  $\mu_B$  becomes large and  $T$  is small, the quantum statistics such as Fermi-Dirac or Bose-Einstein Statistics becomes important. It is remarkable to note that the Bose-Einstein statistics is likely to lead to the Hagedorn condensation when the baryon chemical potential  $\mu_B$  becomes very large at relatively low temperature  $T$ . In this sense the quantum statistics turns to be important.

The grand canonical partition function for the Hagedorn states is given by

$$\begin{aligned}
I &= Z_{(II)}(T, V, \Lambda), \\
&= \exp \left( \int_{m_0}^{\infty} dm \rho_{(II)}(T, \Lambda, m) \left[ \ln z_{(Stats)}(T, m, \Lambda) + \ln z_{(Stats)}(T, m, \Lambda^{-1}) \right] \right), \\
&= Z_{(II)}(T, V, \Lambda; \text{Mesonic}) \times Z_{(II)}(T, V, \Lambda; \text{Baryonic}) \times Z_{(II)}(T, V, \Lambda; \text{Exotic}) \\
&\quad \times (\dots).
\end{aligned} \tag{127}$$

The continuous high-lying mass spectrum can be decomposed to mesonic ( $B = 0$ ) and baryonic ( $B = 1$ ) Hagedorn states and the exotic Hagedorn states with baryonic quantum number  $B > 1$ . The mesonic and baryonic fugacities are given by  $\Lambda_M = e^{(S\mu_S)/T}$  and  $\Lambda_B = e^{(B\mu_B + S\mu_S)/T}$ , respectively, where  $S$  is the strangeness quantum number and  $B$  is the baryonic number. The (ordinary-) baryonic Hagedorns carries  $B = 1$ . The Exotic Hagedorn's states can carry various baryonic and strangeness quantum number  $B = 0, 1, 2, \dots$  etc and  $S = 0, -1, \dots$  etc where the fugacity is reduced to  $\Lambda_{Exotic} = e^{(B\mu_B + S\mu_S)/T}$ . In the case of no strangeness degree of freedom, the strangeness quantum number is reduced to  $S = 0$ . The other flavor degrees of freedom such as charmonium can be introduced in the

same way. The continuous high-lying density of states  $\rho_{(II)}(T, \Lambda, m)$  is decomposed to

$$\begin{aligned}\rho_{(II)}(T, \Lambda, m) &= \sum_S \rho_{(II)}(T, \Lambda_M, m; \text{Mesonic}) \\ &+ \sum_S \rho_{(II)}(T, \Lambda_B, m; \text{Baryonic}) \\ &+ \sum_B \sum_S \rho_{(II)}(T, \Lambda_{Exotic}, m; \text{Exotic}),\end{aligned}\quad (128)$$

where summations are carried over the baryonic and strangeness quantum number  $B$  and  $S$ , respectively. The exotic Hagedorn states are assumed negligible and they are dropped from the calculations. This approximation seems to be reasonable for the hot and diluted matter. Fortunately, the situation is simpler in the case of small  $\mu_B$  and high  $T$  rather than for large  $\mu_B$  and low  $T$ .

The partition functions for mesonic and baryonic Hagedorns read

$$\begin{aligned}\ln Z_{(II)}(\text{Mesonic}) &= \ln Z_{(II)}(T, V, \Lambda_M; \text{Mesonic}), \\ &= \int_{m_0}^{\infty} dm \rho_{(II)}(T, \Lambda_M, m; \text{Mesonic}) \\ &\quad \times [\ln z_{BE}(T, m, \Lambda_M) + \ln z_{BE}(T, m, \Lambda_M^{-1})],\end{aligned}\quad (129)$$

and

$$\begin{aligned}\ln Z_{(II)}(\text{Baryonic}) &= \ln Z_{(II)}(T, V, \Lambda_B; \text{Baryonic}), \\ &= \int_{m_0}^{\infty} dm \rho_{(II)}(T, \Lambda_B, m; \text{Baryonic}) \\ &\quad \times [\ln z_{FD}(T, m, \Lambda_B) + \ln z_{FD}(T, m, \Lambda_B^{-1})],\end{aligned}\quad (130)$$

respectively, where  $m_0$  is determined from the threshold mass  $m_0 = m_{th}$ . The Fermi-Dirac and Boson-Einstein ensembles for the baryonic and mesonic Hagedorns are given in Eqs.(125) and (126), respectively. For example, the mesonic and baryonic fugacities are given by  $\Lambda_M = 1$  in the case of no strange degree of freedom is included (i.e.  $\mu_S = 0$ ) and  $\Lambda_B = e^{\mu_B/T}$ , respectively.

The grand potential for the mesonic and baryonic Hagedorn states are calculated, respectively, as follow

$$\frac{\Omega_{(II)}}{V}(\text{Mesonic Hagedorn gas}) = -T \frac{\partial}{\partial V} \ln Z_{(II)}(\text{Mesonic}), \quad (131)$$

and

$$\frac{\Omega_{(II)}}{V} (\text{Baryonic Hagedorn gas}) = -T \frac{\partial}{\partial V} \ln Z_{(II)} (\text{Baryonic}). \quad (132)$$

In order to simplify the treatment, we follow the standard procedure for heavy Hagedorn states ( $m_0 > 2 \text{ GeV}$ ) those dominates the dilute and hot nuclear matter. The partition functions for classical mesonic and baryonic Hagedorn states, respectively, read

$$\begin{aligned} \ln z_{BE}(T, m, \Lambda_M) &= -(2J_M + 1) V \int \frac{d^3 k}{(2\pi)^3} \ln \left( 1 - \Lambda_M e^{-\sqrt{(k^2 + m^2)}/T} \right), \\ &\approx (2J_M + 1) \Lambda_M V \int \frac{d^3 k}{(2\pi)^3} e^{-\sqrt{(k^2 + m^2)}/T}, \\ &\approx (2J_M + 1) \Lambda_M V \left( \frac{mT}{2\pi} \right)^{3/2} e^{-m/T}, \end{aligned} \quad (133)$$

and

$$\begin{aligned} \ln z_{FD}(T, m, \Lambda_B) &= (2J_B + 1) V \int \frac{d^3 k}{(2\pi)^3} \ln \left( 1 + \Lambda_B e^{-\sqrt{(k^2 + m^2)}/T} \right), \\ &\approx (2J_B + 1) \Lambda_B V \int \frac{d^3 k}{(2\pi)^3} e^{-\sqrt{(k^2 + m^2)}/T}, \\ &\approx (2J_B + 1) \Lambda_B V \left( \frac{mT}{2\pi} \right)^{3/2} e^{-m/T}. \end{aligned} \quad (134)$$

The exotic Hagedorn states with the baryonic number  $B > 1$  are assumed to be suppressed and subsequently they are dropped from the calculations. The classical statistics is an adequate approximation for the flavor invariance when the dilute nuclear matter is heated. However, in the case of the cold and highly compressed nuclear matter, the classical Maxwell-Boltzmann statistic fails for the mesonic Hagedorn states when the meson condensation (in particular the strangeness) takes place in the system. Hence, the exact quantum Bose-Einstein and Fermi-Dirac statistics become essential for cold and dense nuclear matter. The high-lying strangeness condensation takes place when the mesonic Hagedorn frequency approaches zero. This phenomenon takes place when the strange chemical potential  $\mu_S$  reaches a critical value. Hence, under such a circumstance, the Bose-Einstein statistics must be taken exactly in the calculation. Furthermore, the exotic Hagedorn states may turn to be important when the nuclear matter becomes extremely dense in order to soften the equation of state. Fortunately, in the neighborhood of the tri-critical point, the condensation is not expected in the hot and dilute nuclear matter and the classical Maxwell-Boltzmann statistics

remains a good approximation. Hence, the Hagedorn's partition function is approximated to

$$\begin{aligned} \ln Z_{(II)}(T, V, \Lambda) &\approx \frac{V T^{3/2}}{(2\pi)^{3/2}} \sum_Q (2J_Q + 1) \Lambda_Q \int_m^\infty \rho_{(II)}(T, \Lambda_Q, T) m^{3/2} e^{-m/T} dm, \\ &\sim \frac{V T^{3/2}}{(2\pi)^{3/2}} \sum_Q (2J_Q + 1) \Lambda_Q c_Q \int_m^\infty m^{-\alpha_Q + 3/2} e^{-(\frac{1}{T} - b_Q)m} dm, \end{aligned} \quad (135)$$

where  $Q \sim S, B, \dots$  is the Hagedorn's quantum number that is indicated by Eq.(128) and the mass spectral density of the Hagedorn species, namely,  $\rho_Q \sim c_Q m^{-\alpha_Q} e^{b_Q m}$  is identified by its specific internal symmetry as constructed above. The mass spectral exponents  $\alpha_Q \equiv \alpha$  for various symmetries are displayed in Table (I).

The mass spectral density with the conserved charges of the group symmetry  $U(1)_B \times U(1)_S \dots$  (i.e. with a specific flavor symmetry but not the maximal flavor invariance) can be evaluated by adopting the imaginary chemical potentials as follows

$$\rho_{(II)}\left(T, e^{B \frac{\mu_B}{N_c}/T}, e^{S \mu_S/T}, \dots, m\right) \rightarrow \rho_{(II)}\left(e^{iB \Theta_B/N_c}, e^{iS \Theta_S}, \dots, m\right). \quad (136)$$

Therefore, the mass spectral density with the conserved baryon and strange numbers is calculated by finding the Fourier inverse as follows,

$$\rho_{(II)}(B, S, m) = \int_{-\pi}^{\pi} \frac{d\Theta_B}{2\pi} e^{-iB \Theta_B} \int_{-\pi}^{\pi} \frac{d\Theta_S}{2\pi} e^{-iS \Theta_S} \rho_{(II)}\left(e^{iB \Theta_B/N_c}, e^{iS \Theta_S}, m\right). \quad (137)$$

The conservation of the baryon number  $B$  modifies the mass spectral exponent slightly to  $\alpha \rightarrow \alpha + \frac{1}{2}$ . Moreover, the strange degree of freedom (i.e. the conservation of strange number  $S$ ) modifies the mass spectral exponent by an additional term  $m^{-\frac{1}{2}}$  and, subsequently, the resultant mass spectral density becomes  $\rho \sim m^{-(\alpha+1)} e^{b(B, S \dots)m}$  where the explicit formula for  $b(B, S \dots)$  can be calculated using the saddle point approximation. In this case, the partition functions for the mesonic and baryonic Hagedorns are reduced to, respectively,

$$\begin{aligned} \ln Z_{(II)}(\text{mesonic}) &= \int_{m_0}^\infty dm \rho_{(II)}(B=0, S, m) \\ &\times [\ln z_{BE}(T, m, e^{S \mu_S/T}) + \ln z_{BE}(T, m, e^{-S \mu_S/T})], \end{aligned} \quad (138)$$

and

$$\begin{aligned} \ln Z_{(II)}(\text{baryonic}) &= \int_{m_0}^\infty dm \rho_{(II)}(B=1, S, m) \\ &\times [\ln z_{BE}(T, m, e^{\mu_B/T + S \mu_S/T}) + \ln z_{BE}(T, m, e^{-\mu_B/T - S \mu_S/T})]. \end{aligned} \quad (139)$$

The contribution of the liberated gluons due to the modification of the Hagedorn state's internal symmetry is given as follows

$$\ln Z_{lg}(T) = (2J+1) V T^3 N_{lg} \left( \frac{\pi^2}{90} \right), \quad \left( \text{where } J = \frac{1}{2} \right). \quad (140)$$

The liberated gluons due to symmetry reduction is given by  $N_{lg} = 0$ ,  $\frac{1}{2}N_c(N_c+1)$  and  $N_c(N_c-1)$  for unitary, orthogonal and  $U(1)^{N_c}$  Hagedorn states, respectively. The total partition function for the Hagedorn matter becomes

$$\ln Z_{H-matter}(T, V, \Lambda) = \ln Z_{(II)}(T, V, \Lambda) + \ln Z_{lg}(T). \quad (141)$$

## V. CHIRAL PHASE TRANSITION

The role of chiral phase transition can be considered explicitly in the context of the present model [1]. The chiral restoration is expected to take place at the Gross-Witten point or at its neighbourhood but below the point of the color deconfinement. The chiral phase transition is likely to be a first order one if it takes place at the Gross-Witten point [65]. We shall demonstrate in the present section that the chiral phase transition takes place below the deconfinement phase transition point for the orthogonal Hagedorn states. If this is the case, then the standard treatment given in the preceding sections is sufficient. However, if the chiral restoration takes place far away above the Gross-Witten point in the matter that is dominated by the Hagedorn states then the effect of the chiral field becomes important. In this case, the chiral Hagedorn states have to be considered explicitly in the calculation. The contribution of the discrete low-lying hadron mass spectrum is negligible since the nuclear matter at extreme conditions turns to be dominated by the Hagedorn states above the Gross-Witten point. The partition function for the quark and antiquark given by Eq.(21) in the absent of the chiral background is modified when the chiral field is considered in the calculation. In the mean field approximation, Eq.(21) is modified to become

$$\begin{aligned} \ln Z_{q\bar{q}\sigma}(\beta, V, \sigma) = & (2J+1)V \sum_q^{N_f} \int \frac{d^3\vec{p}}{(2\pi)^3} \sum_i \left[ \ln \left( 1 + e^{-\beta(\epsilon_q(\vec{p}, \sigma) - \mu_q - i\frac{\theta_i}{\beta})} \right) \right. \\ & \left. + \ln \left( 1 + e^{-\beta(\epsilon_q(\vec{p}, \sigma) + \mu_q + i\frac{\theta_i}{\beta})} \right) \right], \end{aligned} \quad (142)$$

where  $\epsilon(\vec{p}, \sigma) = \sqrt{\vec{p}^2 + (m_q^*(\sigma))^2}$ ,  $m_q^*(\sigma) = m_q + g_\sigma \sigma$  and  $\sigma = \langle \sigma \rangle$  is the chiral mean field condensate. Hence in the background of the chiral field, the quark-gluon partition function,

in the Hilbert space, reads

$$Z_{q\bar{q}g\sigma}(\beta, V, \sigma) = Z_{q\bar{q}\sigma}(\beta, V, \sigma) \times Z_g(\beta, V). \quad (143)$$

The gluon partition function  $Z_g(\beta, V)$  is given by Eq.(41). The color-singlet state of the mixed-grand canonical ensemble for the chiral quark-gluon bag is projected out in the following way

$$\begin{aligned} Z_{Singlet}(\beta, V, \sigma) &= \int d\mu_G(g) \chi_{Singlet}(g) \times Z_{q\bar{q}g\sigma}(\beta, V, \sigma), \\ &= \int d\mu_G(g) Z_{q\bar{q}g\sigma}(\beta, V, \sigma), \end{aligned} \quad (144)$$

where  $\chi_{Singlet}(g) = 1$  and  $G$  refers to the group classification either unitary, orthogonal or symplectic one. The integration over the invariance Haar measure is performed in the standard way using the Gaussian integration method as that is presented in Sec. II (see also Refs. [1, 2]). Furthermore, the micro-canonical ensemble with large energy  $W$  is calculated by taking the inverse Laplace transform of the mixed-grand canonical ensemble in the following way

$$Z_{Singlet}(W, V, \sigma) = \frac{1}{2\pi i} \int_{\beta_0 - i\infty}^{\beta_0 + i\infty} d\beta e^{\beta W} Z_{Singlet}(\beta, V, \sigma). \quad (145)$$

The inverse Laplace transform is evaluated using the steepest decent method [1, 2]. The Laplace stationary point is determined by extremizing the exponential with respect to the Laplace variable  $\beta$ . Because of the finite value of the quark's chiral mass, the solution of the Laplace saddle point becomes a transcendental one and can not be written in a closed form. In this case, the saddle point and the inverse Laplace transform is evaluated by iteration [1]. The first iteration is sufficient to shed the light on the chiral restoration phase transition. The standard MIT bag model furnishes the following relations between the bag's mass and volume:

$$\begin{aligned} m &= W + BV, \\ W &= \frac{3}{4}m, \\ V &= \frac{m}{4B}, \end{aligned} \quad (146)$$

where  $B$ ,  $W$ ,  $V$  and  $m$  are the bag's constant, cavity energy, volume and mass, respectively. Hence, the Hagedorn's density of states for the chiral color-singlet quark-gluon bag with a specific internal color symmetry is reduced to

$$\rho_H(m, \sigma) \propto Z_{Singlet}(W, V, \sigma)|_{(W=\frac{3}{4}m, V=\frac{m}{4B})}. \quad (147)$$



The mixed-grand canonical ensemble for the matter of chiral Hagedorn states reads

$$\begin{aligned} \ln Z_{(II)}(T, \mu, V, \sigma) &= 2(2J_H + 1) \cosh(\mu_H/T) \\ &\times V \int_{m_0}^{\infty} dm \rho_H(m, \sigma) \left(\frac{mT}{2\pi}\right)^{3/2} e^{-m/T}. \end{aligned} \quad (148)$$

The total grand potential density for the chiral Hagedorn matter in the presence of the chiral field is given by

$$\begin{aligned} \frac{1}{V} \Omega_{\sigma}(T, \mu, V, \sigma) &= -T \frac{\partial}{\partial V} \ln Z_{(II)}(T, \mu, V, \sigma) + U(\sigma), \\ &= \frac{1}{V} \Omega_{H\sigma}(T, \mu, V, \sigma) + U(\sigma). \end{aligned} \quad (149)$$

The chiral Hagedorn's grand potential density ( i.e. the first term on the right hand side of Eq.(149) ) is given as follows,

$$\begin{aligned} \frac{1}{V} \Omega_{H\sigma}(T, \mu, V, \sigma) &= -T \frac{\partial}{\partial V} \ln Z_{(II)}(T, \mu, V, \sigma), \\ &= -2(2J_H + 1) \cosh(\mu_H/T) \\ &\times T \int_{m_0}^{\infty} dm \rho_H(m, \sigma) \left(\frac{mT}{2\pi}\right)^{3/2} e^{-m/T}. \end{aligned} \quad (150)$$

The chiral potential  $U(\sigma)$  ( i.e. the second term on the right hand side of Eq.(149) ) can be introduced by a phenomenological one in the following way

$$U(\sigma) = \frac{1}{2} m_{\sigma}^2 \sigma^2 + \frac{1}{3} c_2 \sigma^3 + \frac{1}{4} c_3 \sigma^4, \quad (151)$$

where the cubic and quartic terms represent the scalar self-interactions and they were proposed by Boguta and Bodmer [66]. In the simplest approximation, the cubic and quartic terms are neglected by taking  $c_2 = 0$  and  $c_3 = 0$  and this corresponds to the Walecka-like models. The value of the mean field  $\sigma$  is determined by calculating the extremum (i.e. minimum) of the total grand potential density, namely,

$$\frac{1}{V} \frac{\partial}{\partial \sigma} \Omega_{\sigma}(T, \mu, V, \sigma) = 0. \quad (152)$$

In order to calculate the chiral Hagedorn's grand potential density that is given in Eq.(150), the high-lying mass spectral density for chiral Hagedorn states is rewritten in the following way

$$\rho_H(m, \sigma) = c m^{-\alpha} e^{b(\sigma)m}. \quad (153)$$

In the context of standard MIT bag model (see for instance Eq.(105)), the exponential term, namely,  $b(\sigma)$  reads

$$b(\sigma) = \frac{1}{B^{1/4}} \left[ \tilde{a}_{q\bar{q}g}^{(0)}(\sigma) \right]^{1/4}. \quad (154)$$

Furthermore, the function  $\tilde{a}_{q\bar{q}g}^{(0)}(\sigma)$  with the chiral field background is determined as follows

$$\tilde{a}_{q\bar{q}g}^{(0)}(\sigma) = \tilde{a}_{q\bar{q}}^{(0)}(\sigma) + \tilde{a}_g^{(0)}, \quad (155)$$

where the chiral quark-antiquark term reads

$$\begin{aligned} \tilde{a}_{q\bar{q}}^{(0)}(\sigma) &= (2J+1)N_c \frac{1}{2\pi^2} \sum_q^{N_f} \int_0^\infty dx x^2 \\ &\quad \times \ln \left[ 1 + 2 \cosh \left( \frac{\mu_q}{T} \right) e^{-\sqrt{x^2 + (\bar{\beta} m_q^*(\sigma))^2}} + e^{-2\sqrt{x^2 + (\bar{\beta} m_q^*(\sigma))^2}} \right], \\ &= (2J+1)N_c \frac{1}{3\pi^2} \sum_q^{N_f} \int_0^\infty dx \frac{x^4}{\sqrt{x^2 + (\bar{\beta} m_q^*(\sigma))^2}} \\ &\quad \times \frac{e^{-\sqrt{x^2 + (\bar{\beta} m_q^*(\sigma))^2}} \left[ e^{-\sqrt{x^2 + (\bar{\beta} m_q^*(\sigma))^2}} + \cosh \left( \frac{\mu_q}{T} \right) \right]}{\left[ 1 + 2 \cosh \left( \frac{\mu_q}{T} \right) e^{-\sqrt{x^2 + (\bar{\beta} m_q^*(\sigma))^2}} + e^{-2\sqrt{x^2 + (\bar{\beta} m_q^*(\sigma))^2}} \right]}. \end{aligned} \quad (156)$$

The gluon term remains intact and is given by  $\tilde{a}_g^{(0)} = (2J+1)N_{adj} \left( \frac{\pi^2}{90} \right)$ . The term  $\tilde{a}_{q\bar{q}}^{(0)}(\sigma) \Big|_{\sigma=0}$  with zero chiral field background is reduced to

$$\begin{aligned} \tilde{a}_{q\bar{q}}^{(0)}(\sigma) \Big|_{\sigma=0} &= \tilde{a}_{q\bar{q}}^{(0)} \\ &= (2J+1)N_c \sum_q^{N_f} \left[ \frac{7\pi^2}{360} + \frac{1}{12} \left( \frac{\mu_q}{T} \right)^2 + \frac{1}{24\pi^2} \left( \frac{\mu_q}{T} \right)^4 \right]. \end{aligned} \quad (157)$$

The saddle point  $\bar{\beta}$  is calculated by iteration with respect to the chiral mean field  $\sigma$ . The first iteration in the context of the MIT bag model leads to ( see also Eq.(104) ),

$$\begin{aligned} \bar{\beta} &= \frac{1}{W} \left[ 3\tilde{a}_{q\bar{q}g}^{(0)} V W^3 \right]^{\frac{1}{4}}, \\ &= \left[ \tilde{a}_{q\bar{q}g}^{(0)} / B \right]^{\frac{1}{4}}. \end{aligned} \quad (158)$$

The mass spectral exponent  $\alpha$  that appears in the mass spectral density that is given in Eq.(153) is determined by Eq.(87). It is reduced to  $\alpha = 3, \frac{9}{2}$  and  $\frac{15}{2}$  for the orthogonal, unitary and symplectic Hagedorn states, respectively. It becomes  $\alpha = \frac{3}{2}$  for  $U(1)^{N_c=3}$  Hagedorn

states. The color-singlet projection with unimodular-like constraint is imposed in the all preceding Hagedorn states. It is reduced to  $\alpha = \frac{1}{2}$  for color non-singlet  $SU(3)$  quark-gluon bags. The values of the mass spectral exponent  $\alpha$  with various symmetries are displayed in Table (I). The variation of the chiral Hagedorn's grand potential density with respect to  $\sigma$  is reduced to

$$\begin{aligned} \frac{1}{V} \frac{\partial}{\partial \sigma} \Omega_{H\sigma}(T, \mu, V, \sigma) &= -2(2J+1) \frac{1}{(2\pi)^{3/2}} T^{5/2} c \left( \frac{\partial b(\sigma)}{\partial \sigma} \right) \\ &\quad \times \int_{m_0}^{\infty} dm m^{-\alpha+5/2} e^{(b(\sigma)-T)m}, \\ &\sim -(\dots) \int_{m_0}^{\infty} dm m^{-\alpha+5/2} e^{(b(\sigma)-T)m}. \end{aligned} \quad (159)$$

The scalar mean field, namely,  $\sigma = \langle \sigma \rangle$  is found by extremizing  $\Omega_{\sigma}(T, \mu, V, \sigma)$  which is presented in Eq.(149). The value of mean field  $\sigma = \sigma_0$  can be approximated to

$$m_{\sigma}^2 \sigma \propto \left( \frac{\partial b(\sigma)}{\partial \sigma} \right) \times \int_{m_0}^{\infty} m^{-\alpha+5/2} e^{(b(\sigma)-T)m} dm. \quad (160)$$

The consequence of Eq.(160) when the temperature reaches the deconfinement one is important. The integral term on the right hand side of Eq.(160) diverges for the mass spectral exponent  $\alpha \leq \frac{5}{2} + 1$ . It implies that the only possible solution is that  $\frac{\partial b(\sigma)}{\partial \sigma} = 0$  and  $\sigma = 0$ . This means that the chiral field is certainly restored before the deconfinement phase transition point is reached. Hence, the chiral symmetry is restored far away below the deconfinement point for nuclear matter that is dominated by the orthogonal Hagedorn states (or the Hagedorn states with mass spectral exponent  $\alpha \leq \frac{5}{2} + 1$ ). On the other hand, it is possible to have a finite value solution for  $\sigma$  for Hagedorn states with mass spectral exponent  $\alpha > \frac{5}{2} + 1$ . Furthermore, when the exponent exceeds the limit  $\alpha > \frac{7}{2} + 1$ , then it is possible to have the first order chiral phase transition simultaneously with the deconfinement phase transition point. This support the existence of the tri-critical point at finite  $\mu_B$  and  $T$  where the nuclear matter at moderate baryonic densities is supposed to be dominated by the unitary Hagedorn states prior the color deconfinement phase transition.

## VI. DISCUSSIONS

In order to study the deconfinement phase transition diagram in QCD, the hadronic density of states must be known for the entire energy domain below the borderline of the

deconfinement phase transition to the true deconfined quark-gluon plasma. The hadronic density of states for the discrete low-lying mass spectrum is found from the available experimental data that is listed in the particle data group book [3]. The discrete low-lying mass spectrum is extrapolated to the continuous high-lying one using reasonable theoretical models. The standard theoretical procedure to find the hadronic density of states is carried out by computing the micro-canonical ensemble for the quark and gluon bag with specific internal symmetry that is consistent with the experimental observation and other theoretical models. The confined quark and gluon state is guaranteed by projecting the color-singlet state (i.e. the colorless state). The structure of the underlying internal color symmetry of a composite bag has attracted much attention in order to understand the confinement/deconfinement in QCD. The Hagedorn model seems to be very useful in studying the shear viscosity of QGP and even investigating the extended gauge (conformal) field theories such as AdS/CFT. The bag's constituent quarks and gluons are considered in the context of various underlying symmetry groups such as the orthogonal, unitary and symplectic symmetry groups as well as  $U(1)^{N_c}$  symmetry group. In order to be consistent with QCD, the unimodular-like constraint is imposed in the all symmetry groups those are under the present investigation. The unimodular-like constraint is an additional constraint for the orthogonal and symplectic symmetry groups and its absence does not affect the general discussion of the present work. Usually, the natural choice in QCD is the unitary symmetry group. Hence, the transmutation from the unitary symmetry group to orthogonal or symplectic symmetry group is associated with a new phenomenology. The major argument is that: is it possible under certain scenario the the Hagedorn matter that is dominated by the colorless unitary states to be altered (by transmutation) to another one dominated by either colorless orthogonal states or colorless symplectic ones and vice versa? It is important to mention here that the Hagedorns are colorless regardless of their internal color symmetries. The colorless is guaranteed by projecting the color-singlet-state. The answer is that: this scenario seems to be reasonable in order to explain the elusive behaviour of the deconfinement quark gluon plasma in the phase transition diagram.

Furthermore, the relevant point to the hadronic phase transition is the Gross-Witten point. This point is associated by modifications in the hadronic matter properties. The Gross-Witten point is strongly believed to be not the deconfinement point and to be merely a transition from hadronic matter that is known to be dominated by the low-lying mass

spectrum to another class of hadronic matter. The Gross-Witten point is interpreted to be the point where the phase transition from the discrete low-lying mass spectrum to the continuous high-lying mass spectrum is taken place in the hadronic matter. The low-lying mass spectrum is defined by the known hadrons those are available and known experimentally while the high-lying mass spectrum is defined by the Hagedorn states. The phase transition from the low-lying to the high-lying hadronic mass spectrum is caused by the modification of the analytical solution for the color-singlet-state of the underlying group structure of a composite bag. The analytical solution for the color-singlet-state is modified drastically when the Vandermonde effective potential develops a virtual singularity. When the solution is regulated, another analytical solution emerges and the hadronic phase transition from the discrete low-lying mass spectrum to the Hagedorn matter takes place in the system. Evidently, the Gross-Witten point differs from the deconfinement phase transition point and it is located in the hadronic phase below the deconfinement's threshold. Therefore, the Gross-Witten point seems to be necessary for the existence of the tri-critical point and the multi-phase transition processes below the deconfined quark-gluon plasma.

The hadronic phase transition from the hadronic matter which is dominated by the discrete low-lying hadronic mass spectrum (consists baryons such as  $N, \Lambda, \Sigma, \Xi, \dots$  and mesons such as pions, kaons,  $\dots$ ) (i.e. all the hadrons that are found in particle data group book [3]) to another hadronic matter that is dominated by the continuous high-lying hadronic mass spectrum (i.e. Hagedorn states) takes place at the Gross-Witten point. It is argued that the hadronic phase transition is of the higher order and it is typically of a third order one. Since the discrete low-lying hadronic mass spectrum below the Gross-Witten point is presumed to maintain the original internal unitary  $SU(N_c)$  structure, it is natural to assume that the initial Hagedorn states which emerge just above the Gross-Witten point is the mass spectrum of a composite bag with colorless  $SU(N_c)$  states. Moreover, it is reasonable under certain conditions to imagine that it is easier for the Hagedorn states to modify their internal symmetry from the unitary  $SU(N)$  representation to either an orthogonal  $O(N)$  symmetry group or a symplectic  $Sp(N)$  symmetry group. The modification of the composite Hagedorn internal symmetry takes place by either the partial symmetry breaking or the partial symmetry restoration rather than breaking the symmetry group entirely from the colorless state to the colored  $SU(N_c)$  state (i.e. color-non-singlet state). Since the discrete low-lying mass spectrum maintains  $SU(N_c)$  symmetry, the continuous

high-lying mass spectrum threshold likely emerges at first as the colorless unitary  $SU(N_c)$  states. The high thermal excitations modify the internal symmetry of the unitary Hagedorn states. Therefore, the continuous high-lying mass spectrum seems to have the feature to modify its own internal symmetry structure and subsequently the mass spectral exponent  $\alpha$ . The difficulty to catch a clean signature of the explosive quark-gluon plasma can be traced to the multi-modifications (or transmutations) of the hadronic phase just below the deconfinement phase transition but above the Gross-Witten transition. Furthermore, the excited exotic matter that can be formed aftermath the proton-proton collisions at LHC can be traced to Gross-Witten phase transition from the low-lying mass spectrum to the Hagedorn states and the subsequent multiple phase transition processes at low baryonic density and high temperature.

The breaking of the quark-gluon bag's internal symmetry from the colorless  $SU(N_c)$  state (i.e. color-singlet state) to the colored  $SU(N_c)$  state (i.e. color-non-singlet state) requires much more energy than that is needed for the Hagedorn state to alter its internal symmetry from the colorless unitary state to the colorless orthogonal state and freeing gluonic jets to the medium due to the reduction in the number of adjoint degrees of freedom in the composite Hagedorn bags. In this sense, the colorless  $SU(N_c)$  bags transmute to orthogonal ones and emit gluonic jets (due to the reduction of the adjoint degrees of freedom) and these jets decay to other (exotic) particles. The resultant colorless orthogonal bags under extreme hot nuclear matter may undergo a direct deconfinement phase transition to the quark-gluon plasma. In this case, the colorless orthogonal state is fully broken to the colored  $SU(N_c)$  symmetry where the colored quarks and gluons are liberated to form deconfined quark-gluon plasma. Hence, it seems that the resultant Hagedorn phase which is dominated by colorless orthogonal quark-gluon bags explains the fluid properties such as the low viscosity for the quark-gluon plasma in the RHIC and possibly in the LHC. The possible explanation is that the effective orthogonal Vandermonde potential is weaker than the unitary one but it still acts as the Coulomb gas or gas of fluid droplets. On the other hand, it is possible to think about the coupling of various degrees of freedom such as the translation, color and flavor degrees of freedom when the nuclear matter is highly compressed. The translation invariance of the flavor quarks might be badly broken in the extreme dense nuclear matter. Hence, it is reasonable to assume that the color symmetry group partially merges with the translation and/or flavor symmetry group and the resulting color-flavor (or color-translation) degrees

of freedom form an effective color-flavor symmetry group. In other words, the colorless unitary (or orthogonal) state couples with flavor degree of freedom  $SU_V(N_f)$  (or  $SO(N_f)$ ) and forms an effective colorless symplectic  $Sp(N)$  state. This new symmetry maintains the maximal flavor invariance (i.e. conserved  $U(1)^{N_f-1}$ ) and guarantees the colorless state (i.e. color-singlet) in a nontrivial way. Hence, the effective symplectic symmetry is basically a coupled color-flavor symmetry. Furthermore, the color symmetry remains colorless when the symplectic  $Sp(N)$  symmetry is projected to the color-singlet state while the flavor symmetry remains to maintain its maximal invariance in the following possible scenario

$$\begin{aligned} SU(N_c)|_{singlet} \times SU_L(N_f) \times SU_R(N_f) &\rightarrow SU(N_c)|_{singlet} \times SU_V(N_f) \\ &\rightarrow Sp(N_c)|_{singlet} \times U(1)^{N_f-1}. \end{aligned} \quad (161)$$

Hence, the extremely dense nuclear matter seems to favor the phase transition from the unitary Hagedorn states to the symplectic Hagedorn states.

The mass spectral exponents for the Hagedorn states with different internal symmetries are displayed in Table (I).

Fig. (1) depicts the phase transition diagram in the  $\mu_B - T$  plane. It is shown that at low temperature the dilute nuclear matter which is dominated by the discrete low-lying hadronic mass spectrum states, such as pions, kaons etc and nucleons, Lambdas etc and so on, forms a gas of free discrete low-lying hadrons. Under certain conditions, those hadrons interact with each others and form nuclear matter (usually in the simplest approximation, the hadrons are treated as ideal gas). When the nuclear matter is heated up and/or compressed, it undergoes higher order Gross-Witten Hagedorn phase transition from the nuclear matter that is dominated by the discrete low-lying mass spectrum hadrons to another nuclear matter that is dominated by the continuous high-lying mass spectrum hadronic (Hagedorn) states. The Gross-Witten line appears as the dotted line (red online) in the lower-left of the phase transition diagram. It is shown that the nuclear matter which is dominated by the discrete low-lying hadrons passes higher order Gross-Witten Hagedorn transition to another nuclear matter that is dominated by the continuous high-lying mass spectrum of the colorless unitary  $SU(N_c)$  quark-gluon bag. The order of the phase transition is likely to be a third order one. The intermediate Hagedorn matter is shown above the Gross-Witten line which appears as the dotted line (left) and below the deconfinement phase transition line which appears as the upper thick solid line. It is evident that the continuous high-lying mass spectrum just above

the Gross-Witten point (i.e. a continuous line in the  $\mu_B - T$  plane) is likely to be dominated by the unitary Hagedorns (i.e. colorless unitary  $SU(N_c)$  states). When the dilute  $SU(N_c)$  Hagedorn matter is heated up, the Hagedorn states mutate their internal symmetry from the colorless  $SU(N_c)$  symmetry to the colorless  $O(N_c)$  symmetry. Nevertheless, the flavor symmetry maintains its optimal invariance in the hot nuclear bath. Hence, the unitary Hagedorn matter undergoes phase transition to another Hagedorn matter that is dominated by the colorless orthogonal  $O(N_c)$  states and becomes orthogonal Hagedorn matter. The phase transition from unitary Hagedorn matter to orthogonal Hagedorn matter is shown by the light dotted line (yellow online) on the top left of the  $\mu_B - T$  phase transition diagram. At higher temperature, the Hagedorn matter that is dominated by the colorless orthogonal states undergoes deconfinement phase transition to the quark-gluon plasma where the color-singlet constraint is broken in order to form colored  $SU(N_c)$  states. When the color singlet constraint is broken badly, the colored quarks and gluons are liberated and/or the quark-gluon bags become colored ones. The order of the deconfinement phase transition is supposed to be varied and it is shown by several gray circles on the top and left of the  $\mu_B - T$  phase transition diagram. Two major factors likely modify the order of phase transition: The first factor comes mainly from the Hagedorn internal symmetry modification to either the colorless  $SU(N_c)$ , colorless  $O(N_c)$  or colorless  $Sp(N_c)$  states. It is also possible to assume that the heat can release most of the gluonic contents of the Hagedorn states and mutates them to the colorless  $U(1)^{N_c}$  quark bags in the case of the dilute nuclear matter where  $\mu_B \approx 0$  (i.e. further reduction in the adjoint degrees of freedom). Eventually, the heat can break the color-singlet constraint and the metastable colored (color-non-singlet-state)  $SU(N_c)$  quark-gluon bags (with initial total zero color charges: i.e. color-neutral bags) emerge in the system. The second factor is actually originated from the deformation of the Hagedorn cavity boundary surface. The situation is completely different when the nuclear system is compressed and cooled to lower temperatures. This is marked by the light dotted line (yellow online) on the lower right side of the  $\mu_B - T$  diagram in particular when the baryonic chemical potential  $\mu_B$  becomes relatively large. The flavor degree of freedom becomes more important albeit the system tends somehow to maintain the optimal flavor invariance and restores the chiral symmetry. Furthermore, the strangeness degree of freedom is essential, though it is not mentioned explicitly throughout the present work. Furthermore, along the  $\mu_B$  direction, the nuclear matter also passes the Gross-Witten Hagedorn phase transition from the hadronic



matter which is dominated by the discrete low-lying mass spectrum hadrons to another one that is dominated by the continuous high-lying mass spectrum Hagedorns. The continuous high-lying mass (and volume) spectrum phase is initially dominated by the colorless  $SU(N_c)$  states in particular just above the onset of the Gross-Witten point. Evidently the system undergoes phase transition to another Hagedorn matter that is populated by colorless  $Sp(N)$  states when the color and flavor degrees of freedom are coupled to form  $Sp(N)$  symmetry group. The phase domain of the new colorless  $Sp(N_c)$  states is immured by the light dotted line (online green) on the lower-right side of the  $\mu_B - T$  diagram. It sounds that the nuclear matter which is dominated by the colorless  $Sp(N)$  states overlaps and matches the color-superconductivity, non-CFL quark liquid and CFL alike phases. The complexity of the color-flavor coupling and the nontrivial  $Sp(N)$  structure increases significantly when the system is compressed to form denser nuclear matter.

Fig. (2) focuses on the flavor symmetry besides the color symmetry. It is shown that the Hagedorn matter is initially dominated by the mesonic Hagedorn states for small  $\mu_B$ . When  $\mu_B$  increases, the baryonic Hagedorn states appear in the system besides the existing mesonic Hagedorn states. It follows from Eq.(137) that mass spectral exponent increases by  $\alpha \rightarrow \alpha + \frac{1}{2}$  when the Hagedorn states attain specific baryonic number and it is also modified by  $\alpha \rightarrow \alpha + \frac{1}{2}$  when the strangeness number is included. The strangeness turns to be important when the system is compressed to larger  $\mu_B$  and is heated up to higher temperature. Furthermore, the Hagedorn matter tends to maintain the optimal flavor invariance in the dilute hot nuclear matter keeping in mind that the Hagedorn states are colorless regardless of the type of the internal color structure symmetry or if the color degrees of freedom are coupled to other degrees of freedom. When the maximum flavor invariance is maintained at high temperature, the classical Maxwell-Boltzmann statistics becomes a good approximation under certain circumstances. The classical statistics approximation also suits the exotic Hagedorn states. It is likely that the hadronic matter which is dominated by the colorless orthogonal states undergoes smooth phase transition to the colored (non-color-singlet)  $SU(N_c)$  quark-gluon matter with initial neutral color charges (i.e. color-neutral) for  $\mu_B \approx 0$  at the critical temperature  $T_c$ . The alternate scenario is that the colorless  $U(1)^{N_c}$  quark bags may emerge above the orthogonal Hagedorn states and below the deconfinement phase transition where the color-singlet constraint of the colorless states is broken and the colored (i.e. color-non-singlet) states appear abundantly in the system. This kind of intermediate

process smoothen the order of the phase-transition remarkably at  $\mu_B \approx 0$ . This process is depicted as the symbol  $*$  in Fig. (2). Nonetheless, it is possible for the colorless orthogonal (or unitary) states to pass the phase transition to metastable colored bags via the following reaction:

$$\text{color-singlet } SU(N_c) \text{ or } O(N_c) \text{ Hagedorns etc} \rightarrow \text{colored } SU(N_c) \text{ plasma.} \quad (162)$$

The overall color charge of each bag remains a color-neutral one (i.e. neutral color charge for  $N_{fun}$  fundamental quarks and  $N_{adj}$  adjoint gluons) before the bags expand and become colored ones and, eventually, form colored quark-gluon plasma. This kind of phase transition is likely supposed to be of higher order and takes place on the left hand side of the tri-critical point which appears in the phase transition diagram. When  $\mu_B$  increases, the flavor structure becomes more rich and complex. The flavor symmetry invariance turns to be broken and involved. Therefore, the complexity of the color-flavor structure increases as the system is compressed and cooled down to lower temperature. The color-flavor internal symmetry is modified in an optimal way minimizing the flavor dependence and maximizing the preservation of the colorless state. This mechanism explain why the quarks avoid to propagate freely in the medium. When  $\mu_B$  becomes significantly large, the complexity of the color-flavor symmetry increases and the  $SU(N_c)$  symmetry couples with the  $SU(N_f) \times SU(N_f)$  symmetry. The internal symmetry of the quark and gluon bag turns to be  $Sp(N_c)$  color-flavor symmetry. At high temperature, both the flavor invariance and the color-singlet constraint (i.e. colorless state) modify the quark-gluon bag's underlying internal symmetry from  $SU(N_c)$  to  $O(N_c)$ . The quarkyonic matter is conjectured to be dominated by the continuous high-lying hadronic states (Hagedorns) with varied symmetries such as the orthogonal, unitary and symplectic ones.

It is shown in Fig. (3) that the mass spectral exponent  $\alpha$  is modified with respect to  $\mu_B$  and  $T$  below the brink of the deconfinement phase transition borderline to the quark-gluon plasma. The Hagedorn's mass spectral exponent  $\alpha$  is small for the dilute and hot hadronic matter. The exponent  $\alpha$  is modified as the hadronic matter is compressed and/or heated. The exponent varies and takes the values  $\alpha_1 \leq \alpha_2 \leq \alpha_3$ . The exponents are reduced to  $\alpha_1 = 3$ ,  $\alpha_2 = 9/2$  and  $\alpha_3 = 15/2$  for the colorless orthogonal, unitary and symplectic Hagedorn states, respectively, when  $N_c = 3$ . The mass spectral exponent for the colorless  $U(1)^{N_c}$  composite states (Hagedorns) is reduced to  $\alpha = 3/2$  for  $N_c = 3$ . Furthermore, the

mass spectral exponent for the finite metastable quark-gluon bag with the colored  $SU(N_c)$  state is reduced to  $\alpha_{non} = 1/2$  (i.e. simply colored  $SU(N_c)$  states). The metastable colored bags are expected to emerge before they expand smoothly and overlap each other and eventually form quark-gluon plasma.

Nonetheless, the fuzzy and center of mass corrections modify the mass spectral exponent  $\alpha$  significantly [2]. The center of mass correction has been introduced by Kapusta [5]. Therefore, it is expected that when the fuzzy and center of mass corrections are considered, the exponents  $\alpha$  for the orthogonal, unitary and symplectic Hagedorn states overlap with each other under certain conditions in the hot and compressed nuclear matter. This leads to a smooth transmutation from certain composite bag's internal symmetry to another one.

The complexity of the color-flavor coupling structure for the large  $\mu_B$  is illustrated in Fig. (4). The color-flavor coupling is simplified drastically by correlating the bag's color and flavor symmetries to form the  $Sp(N)$  symmetry group. The mass spectrum for the color superconductivity physics is simplified drastically by considering the colorless  $Sp(N)$  state. It is evident that the mass spectral exponent  $\alpha$  for the continuous high-lying mass spectrum  $\rho_{(II)} = c m^{-\alpha} e^{bm}$  depends essentially on  $\mu_B$  and  $T$ . The order of phase transition is sensitive to the exponent  $\alpha$ . This sensitivity indicates the existence of the tri-critical point in the phase transition diagram. The order of deconfinement phase transition is found first order for the Hagedorn states with the exponent  $\alpha > \frac{7}{2}$ . The second and third order phase transitions are found for Hagedorn states with exponents  $\frac{7}{2} \geq \alpha > 3$  and  $3 \geq \alpha > \frac{17}{6}$ , respectively. Moreover, the  $n^{th}$  order phase transition takes place for  $\frac{5}{2} + \frac{1}{n-1} \geq \alpha > \frac{5}{2} + \frac{1}{n}$ . There is no direct (explosive) deconfinement phase transition to quark-gluon plasma for the hadronic matter that is populated by Hagedorn states with the mass spectral exponent  $\alpha \leq \frac{5}{2}$ . The phase transition for the Hagedorn states with the mass spectral exponent  $\alpha \leq \frac{5}{2}$  is smooth (i.e. smooth cross-over phase transition). In this case, the Hagedorn bags expand smoothly and they are gently thermally excited without an abrupt phase transition to explosive quark-gluon plasma. If the unitary Hagedorns freeze out they undergo Gross-Witten phase transition to the low-lying mass spectrum hadronic matter. This means that the Hagedorn bags evaporate to the discrete low-lying mass spectrum particles and this resembles the black hole evaporation in AdS/CFT duality.

It is reasonable to assume that the thermal excitation may change the Hagedorn bag's internal structure. For instance under certain circumstances the nuclear matter that is

dominated by the unitary Hagedorn states is altered to be dominated by the orthogonal Hagedorn states when the dilute nuclear matter is heated up to higher temperatures. Since the mass spectral exponent for orthogonal Hagedorns (i.e. colorless orthogonal states) is found to be  $\alpha_1 = 3$ , it is likely that the orthogonal Hagedorn matter undergoes third order phase transition to quark-gluon plasma. Furthermore, it is possible that the orthogonal Hagedorn states are altered to colorless  $U(1)^{N_c}$  states when the very dilute nuclear matter is further heated up to higher temperatures. The very dilute nuclear matter might be created in the  $pp$  collisions at LHC besides the heavy ion collisions. The Hagedorn matter which is dominated by the colorless  $U(1)^{N_c}$  has the mass spectral exponent  $\alpha = 3/2$ . Hence, the nuclear matter that is dominated by these states does not undergo direct abrupt phase transition to quark-gluon plasma but rather smooth cross-over phase transition. When the medium is further heated up to higher temperature these states (i.e. Hagedorn states with the mass spectral exponent  $\alpha = 3/2$ ) may be mutated to metastable colored quark-gluon bags with the mass spectral exponent  $\alpha = 1/2$ . Since the states with mass spectral exponent  $\alpha = 1/2$  do not pass direct explosive deconfinement phase transition to quark-gluon plasma, the colored quark-gluon bags expand smoothly and the system undergoes smooth phase transition to colored quark-gluon plasma.

The orthogonal Hagedorn states are mutated to the colorless  $U(1)^{N_c}$  quark-gluon bags due to the high thermal excitations in the hot and very dilute nuclear matter (i.e.  $\mu_B \approx 0$ ). Since the new nuclear matter turns to be dominated by the colorless  $U(1)^{N_c}$  quark-gluon bags, it does not likely undergo direct phase transition to explosive quark-gluon plasma. But instead, the resultant Hagedorn states are gradually altered to metastable colored quark-gluon bubbles. The metastable colored quark-gluon bags expand gradually and overlap each other smoothly until the entire space is filled by giant colored (non-singlet) bags. The resultant matter have an initial neutral color charge aftermath the phase transition. Therefore, the constraints of the conserved color charges must be embedded in the system through the color chemical potentials. This kind of (color-non-singlet) matter with the mass spectral exponent  $\alpha_{non}$  undergoes a smooth cross-over phase transition to non-explosive quark-gluon plasma. The multi-processes mechanism in the phase transition from the low-lying hadronic phase to the quark-gluon plasma strongly indicates the fluid behaviour for the quark-gluon plasma. The color-singlet states for the quark-gluon bag with an orthogonal color representation rather than the unitary one can be interpreted as a gas of Coulomb

quark-gluon bags (or quark-gluon liquid). Furthermore, the color-singlet states for the quark bag with  $U(1)^{N_c}$  color symmetry group can be argued to be quark rich liquid bags and gluon rich medium. The phase transition to the colorless orthogonal states (i.e. orthogonal Hagedorns) or colorless  $U(1)^{N_c}$  states may explain the fluid properties and the low viscosity factor for the quark-gluon plasma at the RHIC and possibly LHC. This class of phase transition enriches the medium with gluonic jets besides the Hagedorn states. Furthermore, in the case that the orthogonal or  $U(1)^{N_c}$  Hagedorn states freeze out at some point before reaching the quark-gluon plasma, they evaporate to the (exotic-) low-lying mass spectrum particles via Gross-Witten like phase transition in an analogous way to the black holes evaporation in AdS/CFT.

The hot and little compressed hadronic matter ( $\mu_B \neq 0$ ) is likely to be dominated by the orthogonal Hagedorn states above the Gross-Witten point. This kind of nuclear matter tends to undergo higher order phase transition ( for instance third order with  $\alpha=3$  ) to the deconfined quark-gluon plasma. In this case, the color-singlet state of the orthogonal symmetry group is broken smoothly to form the colored  $SU(N_c)$  state (i.e. color-non-singlet state) and, subsequently, the quarks and gluons are liberated. At the intermediate baryonic chemical potential  $\mu_B$ , the continuous high-lying unitary Hagedorn matter undergoes first order phase transition to explosive quark-gluon plasma. The color-singlet state is broken badly to form the colored  $SU(N_c)$  state. The explosive quark-gluon plasma needs much thermal energy to be detonated. Furthermore, it should be noted that when  $\mu_B$  is reduced below a critical value, the unitary Hagedorn states tend to transmute to the orthogonal Hagedorn states prior to the deconfinement phase transition to quark-gluon plasma but this is not the case for the saturate orthogonal Hagedorn matter when  $\mu_B$  increases and exceeds a critical value.

On the other hand, the mass spectral exponents for the unitary and symplectic Hagedorn states are reduced to  $\alpha_2 = 9/2$  and  $\alpha_3 = 15/2$ . This means that the nuclear matter which is dominated by the unitary Hagedorn states likely undergoes direct first order phase transition to the quark-gluon plasma. Furthermore, it is obvious that the symplectic nuclear matter likely undergoes first order phase transition to the explosive quark-gluon plasma when it is heat up.

When the hadronic matter is compressed to the significantly large  $m_B$  and cooled down, the unitary Hagedorn states are mutated to the symplectic ones due to the internal color-

flavor symmetry transmutation. In this case the saturate unitary Hagedorn matter transfers to another nuclear matter that is dominated by the symplectic Hagedorn states. The mass spectral exponent for the symplectic matter is  $\alpha_3 = 15/2$ . The physics of the symplectic Hagedorn matter is very rich. In the context of the present model, the highly dense neutron star turns to be dominated by the symplectic hadronic matter rather than the conventional quark matter in order to soften the equation of state. Furthermore, the existence of the color super-conductivity phases such as the color-flavor locking phase can be interpreted in terms of the the Hagedorn complex internal structure and the color-flavor coupling channel.

In order to understand the microscopic mechanism of the multiple phase transitions from symmetry group to another, the higher order corrections of the hard thermal loops become crucial. Although these corrections are calculated by perturbation, the higher order corrections beyond the one-loop correction are highly non-trivial and also the non-perturbative effect may turn to be essential. The simplest way to understand the symmetry breaking from one group to another is to study the symmetry breaking from  $SU(N_c)$  to  $U(1)^{N_c-1}$ . The program to investigate the local and global symmetry behavior at finite temperature and density such as the symmetry breaking or restoration is a straightforward one. In fact this program relies basically on the dependence of effective mass on the temperature [67, 68]. The symmetry is broken when the effective masses turn to be finite and non-degenerate ones and their corresponding adjoint mean-fields become finite ones when the effect of the higher order terms that are beyond the quadratic part in the effective potential turn to be non-negligible. The gluon effective mass in the present case is defined by the gluon's Debye mass. In order to simplify the discussion to the minimum, the effective potential for the adjoint fields with perturbative corrections beyond the one loop correction will not be considered. Fortunately, the one loop correction sheds some information about what is needed to understand how the symmetry can be broken under extreme conditions. The effective potential for the adjoint fields can be written roughly in the following way

$$\begin{aligned} V_{eff}(\hat{A}_\mu^a) &\doteq \frac{1}{2}\Pi^{\mu\nu a'a}\hat{A}_\mu^{a'}\hat{A}_\nu^a + \frac{1}{3!}\lambda_3^{\mu\nu\kappa abc}\hat{A}_\mu^a\hat{A}_\nu^b\hat{A}_\kappa^c + \frac{1}{4!}\lambda_4^{\mu\mu'\nu\nu'aa'bb'}\hat{A}_\mu^a\hat{A}_{\mu'}^{a'}\hat{A}_\nu^b\hat{A}_{\nu'}^{b'} + \dots, \\ &\doteq \frac{1}{2}\Pi^{\mu\nu a'a}\hat{A}_\mu^{a'}\hat{A}_\nu^a + \frac{1}{4!}\lambda_4^{\mu\mu'\nu\nu'aa'bb'}\hat{A}_\mu^a\hat{A}_{\mu'}^{a'}\hat{A}_\nu^b\hat{A}_{\nu'}^{b'} + \dots, \end{aligned} \quad (163)$$

where  $\Pi^{\mu\nu a'a} \doteq \langle \Pi^{\mu\nu a'a}(p_0, \vec{p}) \rangle$  is the gluon polarization tensor and  $\lambda_4^{\mu\mu'\nu\nu'aa'bb'}$  is the quartic gluon coupling tensor. The quartic gluon coupling tensor can be calculated from the perturbation but also the non-perturbation effect may become signification. The quartic part in

the effective potential is the decisive term in determining the process of the symmetry transmutation (or breaking) [67, 68]. The gluon polarization tensor in the HTL approximation is found [69]

$$\begin{aligned}\Pi_{\mu\nu}{}^{a'a}(p_0, \vec{p}) &= (\mathbf{m}_D^2)^{a'a} \left[ -\delta_\mu^0 \delta_\nu^0 + p_0 \int \frac{d\Omega_k}{4\pi} \frac{\hat{k}_\mu \hat{k}_\nu}{p_0 - \hat{k} \cdot \vec{p}} \right], \\ &= (\mathbf{m}_D^2)^a \delta^{a'a} \left[ -\delta_\mu^0 \delta_\nu^0 + p_0 \int \frac{d\Omega_k}{4\pi} \frac{\hat{k}_\mu \hat{k}_\nu}{p_0 - \hat{k} \cdot \vec{p}} \right].\end{aligned}\quad (164)$$

The information that is needed to understand the Higgs mechanism and symmetry breaking is decoded implicitly in the gluon Debye mass(es). The Debye mass is found as follows

$$\begin{aligned}(\mathbf{m}_D^2)^{a'a} &= (\mathbf{m}_D^2)^a \delta^{a'a}, \\ &= [(\mathbf{m}_{D(Q)}^2)^a + (\mathbf{m}_{D(G)}^2)^a] \delta^{a'a}, \\ &= [\mathbf{t}_{ij}^{a'} \mathbf{t}_{ji}^a (\mathbf{m}_{D(Q)}^2)_i + \mathbf{T}_{cb}^{a'} \mathbf{T}_{bc}^a (\mathbf{m}_{D(G)}^2)^b] \delta^{a'a},\end{aligned}\quad (165)$$

where

$$(\mathbf{m}_{D(Q)}^2)_i = 2 \frac{g^2}{\pi^2} \sum_{Q=1}^{N_f} \left[ \frac{\pi^2}{6} T^2 + \frac{1}{2} (\mu_Q + \mu_{C_i})^2 \right], \quad (166)$$

while the real gluonic part reads

$$\begin{aligned}(\mathbf{m}_{D(G)}^2)^{\underbrace{b=(AB)}} &\rightarrow \Re e (\mathbf{m}_{D(G)}^2)^{\underbrace{b=(AB)}}, \\ &= \frac{g^2}{\pi^2} \left[ \frac{\pi^2}{3} T^2 - \frac{1}{2} (\mu_C^b)^2 \right], \\ &= \frac{g^2}{\pi^2} \left[ \frac{\pi^2}{3} T^2 - \frac{1}{2} (\mu_{CA} - \mu_{CB})^2 \right].\end{aligned}\quad (167)$$

Eq.(165) hints some information about the possible symmetry breaking processes. There is  $(N_c^2 - N_c)$  non-degenerate masses and  $(N_c - 1)$  degenerate masses. It is naively to conjecture that  $\hat{A}^a \propto \mu_C^a \equiv (\mu_{CA} - \mu_{CB})$  where  $a = \underbrace{(AB)}$ . This means that the  $N_c^2 - N_c$  non-degenerate masses correspond the non-vanishing values  $\hat{A}^a$  with  $A \neq B$  while the  $N_c - 1$  degenerate masses correspond  $\hat{A}^a = 0$  with  $A = B$ . Hence the  $N_c^2 - N_c$  non-degenerate masses are simply the Higgs masses which are generated by breaking the symmetry  $SU(N_c)$  while the  $N_c - 1$  degenerate masses are the elements of the resultant new symmetry  $U(1)^{N_c-1}$ . These masses in one (Hard-thermal) loop correction are of order  $m_D \sim gT$ . Depending on the higher order interaction  $(\hat{A}_\mu^a)^{n>2}$  which appear in Eq.(163) and its modification

with temperature and density, it is naturally to surmise multiple phase transitions such as  $SU(N_c) \rightarrow SU(N_c - 1) \times U(1) \rightarrow \cdots \rightarrow U(1)^{N_c-1}$  (see for instance Ref. [70]). More recent discussions of the Higgs mechanism in the semi-quark-gluon plasma can be found in Ref. [71] and the references therein. Instead of breaking the symmetry  $SU(N_c) \rightarrow SU(N_c - 1) \times U(1)$ , the symmetry transmutation undergoes multiple symmetry breaking transitions to  $SU(N_c) \rightarrow O(N_c) \rightarrow SU(N_c - 1) \times U(1)$  in order to maintain the quark confinement. The intermediate symmetry transmutation  $O(N_c)$  smoothes the symmetry breaking from  $SU(N_c)$  to  $U(1)^{N_c-1}$  in order to soften the Hagedorn's equation of state. On the other hand, the microscopic mechanism in the multi-processes for the formation of symplectic symmetry  $Sp(N_c)$  is rather more complicated because of the correlation between the flavor and color symmetries. The symmetry reduction undergoes multiple processes, namely,  $SU_V(N_f) \times SU(N_c) \rightarrow O(2N_c) \times \cdots \rightarrow Sp(N_c)$ . In the process of forming the symmetry  $Sp(N_c)$ , the color degrees of freedom favor to couple the flavor degrees of freedom through anti-symmetric channels to form diquark condensates and energy gaps. The adjoint mean-fields acquire degenerate/non-degenerate effective gluon masses depending of the type of the color superconductivity that is formed in the medium. The symmetry breaking leads to massless Nambu-Goldstone bosons which come from flavor sector and massive gluons which stem from the color sector. In principle, the energy gaps of the color-superconductivity can be included explicitly in the calculation of the canonical ensemble. The multiple symmetry breaking processes from the matter that is dominated by  $SU(N_c)$  Hagedorn states to another one that is dominated by  $U(1)^{N_c-1}$  and the corresponding Higgs mechanism is sketched in Fig.(5). In order to simplify the present work, we assume that the liberated gluons are approximated to an ideal gas of massless particles. In this approximation, the gluon effective masses which are acquired through the symmetry breaking process are neglected and this does not change the conclusion of the possible multiple phase transitions.

## VII. CONCLUSION

The present work is intended to determine the physics behind the intermediate processes toward the quark-gluon plasma in the  $\mu_B - T$  phase transition diagram and the variation of the mass spectral exponent for the Hagedorn mass spectral density in the medium. The  $\mu_B - T$  phase transition diagram from the Hadronic phase to the quark-gluon plasma is



rich and the multiple intermediate transition processes are found essential. The nuclear matter which is dominated by the unitary Hagedorn states passes different phase transitions with different orders depending on the nuclear medium's temperature and density. The dilute nuclear matter that is enriched with the unitary Hagedorn states undergoes phase transition to another matter that is dominated by the orthogonal Hagedorn states when the medium is heated up while the extreme dense nuclear matter that is dominated by the unitary Hagedorn states passes phase transition to another one that is dominated by the symplectic Hagedorn states when the medium is further compressed and cooled down. It should be noted that the Hagedorn states are colorless (by projecting only the color-singlet states) regardless of their internal symmetry group. Furthermore, it is possible to imagine under the assumption of certain scenarios that the Hagedorn states passes smooth multiple phase transitions to a neutral color gas of metastable colored bags at  $T \approx T_c$  and  $\mu_B \approx 0$ .

The tri-critical point in the  $\mu_B - T$  phase transition diagram and the fluid behaviour of the quark-gluon plasma at a low baryonic chemical potential  $\mu_B$  and high temperature  $T \gg 0$  can be interpreted in terms of the modification of the Hagedorn mass spectral density due to the modification in the quark-gluon bag's internal symmetry. At low temperature, the nuclear matter is dominated by the discrete low-lying mass spectrum (hadrons) and when the system is heated up it undergoes higher order phase transition to new nuclear matter that is dominated by the continuous high-lying mass spectrum particles (i.e. Hagedorns). When the Hagedorn states freeze out they evaporate to the discrete low-lying particles through Gross-Witten phase transition in an analogous way to the fragmentation of the big soap bubble to many tiny bubbles.

The Hagedorn states are determined basically by the mass spectrum of the quark and gluon bag with a specific internal symmetry. The color-singlet constraint which guarantees the colorless quark-gluon bags plays an essential role in keeping quarks and gluons confined. The continuous high-lying hadronic matter is dominated at first by the unitary Hagedorn states just above the Gross-Witten point (it appears as a line in  $\mu_B - T$  plane) for the phase transition from the discrete low-lying hadronic matter to the continuous high-lying one. The mass spectral exponent  $\alpha$  of the continuous high-lying mass spectral density  $\rho_{(II)}(m) = c m^{-\alpha} e^{bm}$  depends on the underlying internal symmetry of the Hagedorn bag. The composite bag's internal symmetry is modified from the colorless unitary state to the colorless orthogonal state in the RHIC and/or LHC energy at high temperature. On the

other hand, the quark and gluon bag's internal structure is mutated from the colorless unitary state (unitary Hagedorn) to the colorless symplectic state (symplectic Hagedorn) under the extreme compressed nuclear matter (i.e. when the unitary Hagedorn matter becomes saturated) such that one is found in the compact stars. It is evident that the mass spectral exponent  $\alpha$  increases with respect to  $\mu_B$  when the system is compressed and cooled down. This exponent decreases when the system is heated up. The Hagedorn states which are expected to be produced in the ultra-relativistic heavy ion collisions and beyond have a rather low mass spectral exponent. In the RHIC or LHC energy, it is expected that the dilute hadronic matter which is dominated at first by the unitary Hagedorn states at small  $\mu_B$  passes Hagedorn phase transition to another nuclear matter that is dominated by the orthogonal Hagedorns when the medium is heated up to higher temperature. The resultant orthogonal Hagedorn matter acts as the Coulomb liquid.

At small baryonic density, the hot nuclear matter which is dominated by the colorless orthogonal (Hagedorn) states undergoes higher order phase transition to the colored  $SU(N_c)$  states with total color-neutral quark-gluon plasma. The colored  $SU(N_c)$  states are colored quark-gluon bags (i.e.: color-non-singlet states). The conserved color charges are adjusted by the color chemical potentials. The colored quark-gluon bags with color-non-singlet states are not Hagedorn states. Aftermath the deconfinement phase transition, the medium is enriched by colored quarks and gluons. In this sense the bag's color-singlet constraint is badly broken and the bag becomes a colored one where the colored quarks can be liberated or exchanged.

The phase transition from the hadronic matter which is dominated by the colorless Hagedorns to another matter that is populated by the colored bags is associated with the breaking of the color-singlet constraint. The breaking of Hagedorn bag's internal symmetry from the color-singlet state of the unitary symmetry to the colored unitary state probably takes place through several intermediate processes in the following way:

$$\begin{aligned}
\text{colorless } SU(N_c) &\rightarrow \text{colorless } O_{(S)}(N_c) + \frac{1}{2}N_c(N_c + 1) \text{ gluons,} \\
&\rightarrow \text{colorless } U(1)^{N_c} + N_c(N_c - 1) \text{ gluons,} \\
&\rightarrow \text{colored } SU(N_c) \text{ (i.e. color-non-singlet states),} \\
&\rightarrow N_c \text{ quarks} + (N_c^2 - 1) \text{ gluons,}
\end{aligned} \tag{168}$$

where the unimodular-like constraint is imposed in all the symmetries are involved in the

present study. In fact, there is  $N_c^2$  adjoint degrees of freedom in the  $U(N_c)$  unitary representation and the unimodular constraint reduces the number of degree of freedom by one. When the Hagedorn's internal structure is mutated from the colorless unitary state to the colorless orthogonal state, the number of (Hagedorn's internal) adjoint gluon degrees of freedom is reduced from  $N_c^2$  to  $N_c(N_c + 1)/2$ , respectively. Therefore, the  $N_c(N_c - 1)/2$  free colorless gluons escape from the Hagedorn bag and emerge in the medium as jets. The nuclear matter turns to be dominated by the orthogonal Hagedorns and is enriched by gluonic content. The  $N_c(N_c - 1)/2$  gluon species may glue together and probably emerge as color-neutral glueballs or jets. When the temperature  $T$  increases, the surfaces of colored bags are perturbed and expand by the thermal excitations and the system undergoes smooth phase transition to true deconfined quark-gluon plasma. The higher order phase transition is not usually associated with the explosive quark-gluon plasma. Moreover, it seems that the colored bags that emerge through smooth phase transition are rather mechanically stable. Hence the preceding scenario leads to smooth cross-over phase transition to quark-gluon plasma at  $\mu_B \approx 0$  and high  $T$  and on the left hand side of the tri-critical point. In the present approximation, the liberated gluons are considered as an ideal gas of massless particles. However, the breaking of the Hagedorn's internal symmetry from the unitary symmetry to the orthogonal one may breaks the color global part of the liberated gluons and they acquire finite mass through the Higgs mechanism. This mechanism will suppress the contribution of the gluon's partition function in particular if the liberated gluons attain large masses.

On the other hand, when the system is compressed and cooled down, the higher order phase transition is reduced to the first order one at the moderate nuclear density. This takes place as  $\mu_B$  increases and exceeds the tri-critical point (i.e. on the right hand side of the tri-critical point). The system prefers to be dominated by the unitary Hagedorns in the stripe above the Gross-Witten point and below the quark-gluon plasma. When the medium becomes denser and hotter, the unitary Hagedorn states will not transmute to orthogonal Hagedorn states anymore but instead they become rather mechanically unstable and the system prefers to pass direct deconfinement phase transition to quark-gluon plasma. Due to the high thermal excitations, they likely pass the first order transition to quark-gluon plasma. This kind of phase transition breaks badly the color-singlet constraint and subsequently the colored  $SU(N_c)$  symmetry becomes possible. Therefore, the system undergoes first order deconfinement phase transition to explosive quark-gluon plasma at moderate  $\mu_B \neq 0$ . Unlike

the smooth cross-over phase transition which usually takes place at small baryonic density (i.e.  $\mu_B \approx 0$ ), the color charges are capable to escape and subsequently the color neutrality is violated. In this case, the color-singlet constraint is loosed and the bag's internal symmetry is broken violently above the right hand side of the tri-critical point in the following way:

$$\text{colorless: color-singlet } SU(N_c) \rightarrow \text{colored } SU(N_c). \quad (169)$$

When the system is compressed and cooled down further more and becomes extremely dense and saturated (i.e.  $\mu_B$  becomes significantly large), the unitary Hagedorn matter transmutes to another one that is dominated by the symplectic Hagedorn states due to the modification of the quark and gluon bag's internal structure and the coupling of color symmetry with other symmetries such as but not limited to the flavor symmetry as follows

$$SU(N_c) \times SU_L(N_f) \times SU_R(N_f) \rightarrow Sp(N) \times \left[ \text{conserved: } U(1)^{N_f-1} \right]. \quad (170)$$

In fact the symplectic symmetry restores additional  $N^2 - N$  adjoint degrees of freedom (for instance partially breaking the flavor invariance  $SU(N_f) \times SU(N_f)$  and leaving  $U(1)^{N_f-1}$  invariance) besides the original  $N_c^2 - 1$  adjoint color degrees of freedom. The phase transition from the unitary Hagedorns to the colorless symplectic states (i.e. symplectic Hagedorns) may take place through more complicated multi-processes in the Hagedorn matter. Furthermore, the mass spectral exponent  $\alpha$  will continue to increase when additional symmetries are incorporated as the nuclear matter becomes denser. Probably, the Hagedorn matter with a certain complex internal symmetry passes to a new physics regime such as forming fluid of stable black holes or dark matter. The deformation of the quark and gluon bag's boundary surface besides other corrections such as the center of mass correction modify the mass spectral exponent  $\alpha$  smoothly. The smooth modification of the mass spectral exponent  $\alpha$  guarantees the continuity of various hadronic phases which are dominated by orthogonal, unitary and symplectic etc Hagedorns. Moreover, it is worth to mention that the symplectic Hagedorn matter is very rich due to the color-flavor coupling or color-angular coupling etc. The emergence of the color-superconductivity and other related physics can be explained in terms of the complex internal structure such as the symplectic Hagedorn matter.

The analysis of the chiral phase transition at low  $\mu_B$  and high  $T$  demonstrates that in the case of the mass spectral exponent  $\alpha \leq 7/2$  such as the mass spectrum for orthogonal Hagedorn states, the chiral restoration phase transition takes place far away below the deconfinement phase transition but at the threshold or above Gross-Witten point. Therefore,

the chiral mass is generated through the multiple phase transition processes from the orthogonal Hagedorn states to the unitary Hagedorn states and subsequently to the low-lying mass spectrum states at the Gross-Witten point.

The order and shape of the  $(\mu_B - T)$  phase transition diagram depends basically on the internal structure of the quark and gluon bags such as but not limited to the color, flavor and angular symmetries. The Hagedorn's mass spectral exponent  $\alpha$  is found to depend essentially on the medium. Furthermore, the multi-intermediate processes in the phase transition diagram from the low-lying hadrons to the eventual quark-gluon plasma is found very rich and not trivial. The complexity of the multi-process phase transitions increases along the temperature axis with the rather small baryonic chemical potential  $\mu_B \sim 0$  (i.e. dilute nuclear matter). It is evident that the Hagedorn's internal structure is significantly modified with respect to both  $T$  and  $\mu_B$ . The mass spectral exponent seems to increase significantly at large baryonic density  $\mu_B \gg 0$  and relatively low temperature (i.e. the extreme dense nuclear matter that is relevant to the compact stars). The order and shape of the phase transition is basically medium dependent. It is associated with complicated multi-processes of symmetry reconfiguration along the chemical potential  $\mu_B$  and temperature  $T$  axes. Therefore, the QCD phase transition diagram is proved to be very rich, tricky and non-trivial one.

## Acknowledgments

The partial support from Alexander von Humboldt foundation is acknowledged.

- 
- [1] I. Zakout and C. Greiner, Phys. Rev. **C78**, 034916 (2008), arXiv:0709.0144 [nucl-th] [nucl-th].
  - [2] I. Zakout, C. Greiner, and J. Schaffner-Bielich, Nucl. Phys. **A781**, 150 (2007), arXiv:nucl-th/0605052.
  - [3] C. Amsler *et al.* (Particle Data Group), Phys. Lett. **B667**, 1 (2008).
  - [4] J. I. Kapusta, Phys. Rev. **D23**, 2444 (1981).
  - [5] J. I. Kapusta, Nucl. Phys. **B196**, 1 (1982).
  - [6] D. J. Gross and E. Witten, Phys. Rev. **D21**, 446 (1980).
  - [7] A. Andronic *et al.* (2009), arXiv:0911.4806 [hep-ph] [hep-ph].

- [8] C. B. Lang, P. Salomonson, and B. S. Skagerstam, Nucl. Phys. **B190**, 337 (1981).
- [9] S. I. Azakov, P. Salomonson, and B. S. Skagerstam, Phys. Rev. **D36**, 2137 (1987).
- [10] O. Aharony, J. Marsano, S. Minwalla, K. Papadodimas, and M. Van Raamsdonk, Adv. Theor. Math. Phys. **8**, 603 (2004), arXiv:hep-th/0310285.
- [11] A. Dumitru, Y. Hatta, J. Lenaghan, K. Orginos, and R. D. Pisarski, Phys. Rev. **D70**, 034511 (2004), arXiv:hep-th/0311223.
- [12] A. Dumitru, J. Lenaghan, and R. D. Pisarski, Phys. Rev. **D71**, 074004 (2005), arXiv:hep-ph/0410294.
- [13] A. Dumitru, R. D. Pisarski, and D. Zschiesche, Phys. Rev. **D72**, 065008 (2005), arXiv:hep-ph/0505256.
- [14] M. L. Mehta, *Random Matrices and the Statistical Theory of Energy Levels* (Academic Press Inc, 1967).
- [15] Y. Nambu, B. Bambah, and M. Gross, Phys. Rev. **D26**, 2875 (1982).
- [16] B. Bambah, Phys. Rev. **D29**, 1323 (1984).
- [17] M. Gross, Phys. Rev. **D27**, 432 (1983).
- [18] S. Jaimungal and L. D. Paniak, Nucl. Phys. **B517**, 622 (1998), arXiv:hep-th/9710044.
- [19] C. R. Gattringer, L. D. Paniak, and G. W. Semenoff, Annals Phys. **256**, 74 (1997), arXiv:hep-th/9612030.
- [20] R. Hagedorn, Nuovo Cim. Suppl. **3**, 147 (1965).
- [21] S. C. Frautschi, Phys. Rev. **D3**, 2821 (1971).
- [22] N. Cabibbo and G. Parisi, Phys. Lett. **B59**, 67 (1975).
- [23] R. Dashen, S.-K. Ma, and H. J. Bernstein, Phys. Rev. **187**, 345 (1969).
- [24] K. Huang and S. Weinberg, Phys. Rev. Lett. **25**, 895 (1970).
- [25] S. Fubini and G. Veneziano, Nuovo Cim. **A64**, 811 (1969).
- [26] V. V. Begun, M. I. Gorenstein, and W. Greiner, J. Phys. **G36**, 095005 (2009), arXiv:0906.3205 [nucl-th] [nucl-th].
- [27] M. I. Gorenstein, M. Gazdzicki, and W. Greiner, Phys. Rev. **C72**, 024909 (2005), arXiv:nucl-th/0505050.
- [28] M. I. Gorenstein, W. Greiner, and S. N. Yang, J. Phys. **G24**, 725 (1998).
- [29] L. Ferroni and V. Koch, Phys. Rev. **C79**, 034905 (2009), arXiv:0812.1044 [nucl-th] [nucl-th].
- [30] R. Abir and M. G. Mustafa(2009), arXiv:0905.4140 [hep-ph] [hep-ph].

- [31] S. Pal(2010), arXiv:1001.1585 [nucl-th].
- [32] J. Noronha-Hostler, M. Beitel, C. Greiner, and I. Shovkovy(2009), arXiv:0909.2908 [nucl-th] [nucl-th].
- [33] J. Noronha-Hostler, C. Greiner, and I. A. Shovkovy, Phys. Rev. Lett. **100**, 252301 (2008), arXiv:0711.0930 [nucl-th] [nucl-th].
- [34] J. Noronha-Hostler, J. Noronha, and C. Greiner, Phys. Rev. Lett. **103**, 172302 (2009), arXiv:0811.1571 [nucl-th] [nucl-th].
- [35] J. Noronha-Hostler, H. Ahmad, J. Noronha, and C. Greiner(2009), arXiv:0906.3960 [nucl-th] [nucl-th].
- [36] Y. Sakai, K. Kashiwa, H. Kouno, and M. Yahiro, Phys. Rev. **D78**, 036001 (2008), arXiv:0803.1902 [hep-ph] [hep-ph].
- [37] H. Abuki, R. Anglani, R. Gatto, G. Nardulli, and M. Ruggieri, Phys. Rev. **D78**, 034034 (2008), arXiv:0805.1509 [hep-ph] [hep-ph].
- [38] K. Fukushima, Phys. Rev. **D77**, 114028 (2008), arXiv:0803.3318 [hep-ph] [hep-ph].
- [39] B.-J. Schaefer, J. M. Pawłowski, and J. Wambach, Phys. Rev. **D76**, 074023 (2007), arXiv:0704.3234 [hep-ph] [hep-ph].
- [40] B. Klein, D. Toublan, and J. J. M. Verbaarschot, Phys. Rev. **D68**, 014009 (2003), arXiv:hep-ph/0301143.
- [41] J. B. Kogut, M. A. Stephanov, D. Toublan, J. J. M. Verbaarschot, and A. Zhitnitsky, Nucl. Phys. **B582**, 477 (2000), arXiv:hep-ph/0001171.
- [42] A. M. Halasz, A. D. Jackson, R. E. Shrock, M. A. Stephanov, and J. J. M. Verbaarschot, Phys. Rev. **D58**, 096007 (1998), arXiv:hep-ph/9804290.
- [43] L. McLerran and R. D. Pisarski, Nucl. Phys. **A796**, 83 (2007), arXiv:0706.2191 [hep-ph] [hep-ph].
- [44] K. A. Bugaev(2009), arXiv:0909.0731 [nucl-th] [nucl-th].
- [45] K. A. Bugaev, V. K. Petrov, and G. M. Zinovjev(2009), arXiv:0904.4420 [hep-ph] [hep-ph].
- [46] K. A. Bugaev, V. K. Petrov, and G. M. Zinovjev, Europhys. Lett. **85**, 22002 (2009), arXiv:0812.2189 [nucl-th] [nucl-th].
- [47] K. A. Bugaev, V. K. Petrov, and G. M. Zinovjev, Phys. Rev. **C79**, 054913 (2009), arXiv:0807.2391 [hep-ph] [hep-ph].
- [48] K. A. Bugaev, V. K. Petrov, and G. M. Zinovjev(2008), arXiv:0801.4869 [hep-ph] [hep-ph].

- [49] K. A. Bugaev, Phys. Rev. **C76**, 014903 (2007), arXiv:hep-ph/0703222.
- [50] R. Stock(2009), arXiv:0909.0601 [nucl-ex] [nucl-ex].
- [51] P. de Forcrand and O. Philipsen, Nucl. Phys. **B642**, 290 (2002), arXiv:hep-lat/0205016.
- [52] Z. Fodor and S. D. Katz(2009), arXiv:0908.3341 [hep-ph] [hep-ph].
- [53] V. I. Yukalov and E. P. Yukalova, Phys. Part. Nucl. **28**, 37 (1997), arXiv:hep-ph/9709338.
- [54] N. Itoh, Prog. Theor. Phys. **44**, 291 (1970).
- [55] J. I. Kapusta and C. Gale, *Finite-Temperature Field Theory: Principles and Applications* (Cambridge University Press, 2006).
- [56] R. Balian and C. Bloch, Ann. Phys. **60**, 401 (1970).
- [57] R. Balian and C. Bloch, Annals Phys. **69**, 76 (1972).
- [58] H. T. Elze, W. Greiner, and J. Rafelski, Phys. Lett. **B124**, 515 (1983).
- [59] H. T. Elze and W. Greiner, Phys. Rev. **A33**, 1879 (1986).
- [60] M. I. Gorenstein, S. I. Lipskikh, V. K. Petrov, and G. M. Zinovev, Phys. Lett. **B123**, 437 (1983).
- [61] G. Auberson, L. Epele, G. Mahoux, and F. R. A. Simao, J. Math. Phys. **27**, 1658 (1986).
- [62] H.-T. Elze, W. Greiner, and J. Rafelski, Z. Phys. **C24**, 361 (1984).
- [63] H. T. Elze and W. Greiner, Phys. Lett. **B179**, 385 (1986).
- [64] H. T. Elze, D. E. Miller, and K. Redlich, Phys. Rev. **D35**, 748 (1987).
- [65] J. B. Kogut, M. Snow, and M. Stone, Nucl. Phys. **B200**, 211 (1982).
- [66] J. Boguta and A. R. Bodmer, Nucl. Phys. **A292**, 413 (1977).
- [67] S. Weinberg, Phys. Rev. **D9**, 3357 (1974).
- [68] L. A. Dolan and R. Jackiw, Phys. Rev. **D9**, 3320 (1974).
- [69] I. Zakout(2010), arXiv:1003.2018 [nucl-th].
- [70] S. Bronoff and C. P. Korthals Altes, Phys. Lett. **B448**, 85 (1999), arXiv:hep-ph/9811243.
- [71] A. Dumitru, Y. Guo, Y. Hidaka, C. P. K. Altes, and R. D. Pisarski(2010), arXiv:1011.3820 [hep-ph].



TABLE I: The mass spectral exponent  $\alpha$  which appears in  $\rho_{(II)} = c m^{-\alpha} e^{bm}$  for the color-singlet state bag (i.e. Hagedorn state) versus the bag's internal symmetry that is given by the  $U(1)^{N_c}$ , orthogonal  $O(N_c)$ , unitary  $U(N_c)$  and symplectic  $Sp(N)$  ( $N = N_c$ ) symmetry groups and they are restricted to the unimodular-like constraint. The exponent  $\alpha$  for the color-non-singlet quark-gluon bags (i.e. colored  $SU(N_c)$ ) state is included.

Symmetry group	$\alpha(N_c)$	$\alpha (N_c = 3)$
Non-singlet $SU(N_c)$ state (not Hagedorn state):	$\frac{1}{2}$	$\frac{1}{2}$
Color-singlet unimodular-like $U(1)^{N_c}$ :	$\frac{1}{2}N_c$	$\frac{3}{2}$
Color-singlet unimodular-like orthogonal $O_{(S)}(N_c)$ : $\frac{1}{4}(N_c^2 + N_c)$		3
Color-singlet unimodular-like unitary $U(N_c)$ :	$\frac{1}{2}N_c^2$	$\frac{9}{2}$
Color-singlet unimodular-like symplectic $Sp(N_c)$ :	$N_c^2 - \frac{1}{2}N_c$	$\frac{15}{2}$

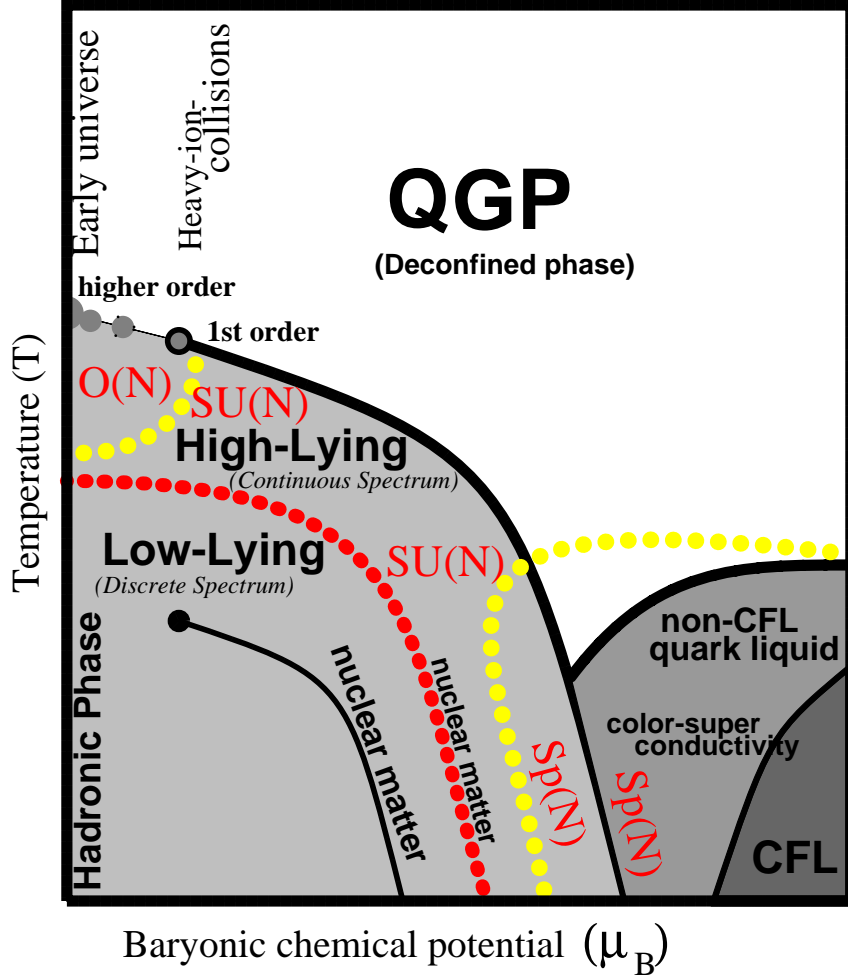


FIG. 1: (Color online) The sketch for the order and shape of the phase transition diagram ( $\mu_B$ - $T$ ) outlining the phase transition between the hadronic matter which is dominated by the discrete low-lying mass spectrum to another one that is dominated by the continuous high-lying mass spectrum and the phase transition from the hadronic phase to the deconfined quark-gluon-plasma. The contiguity of the the discrete low-lying mass spectrum and the continuous high-lying mass spectrum is indicated by the lower-left red dotted line. The Hagedorn phase that is dominated by the continuous high-lying mass spectrum states splits into three individual phases that are dominated by  $SU(N)$ ,  $O(N)$  and  $Sp(N)$  internal color structures. The conventional phase transition diagram for the color superconductivity and color-flavor locked phase is depicted. The color-superconductivity phase falls under the  $Sp(N)$  group domain.



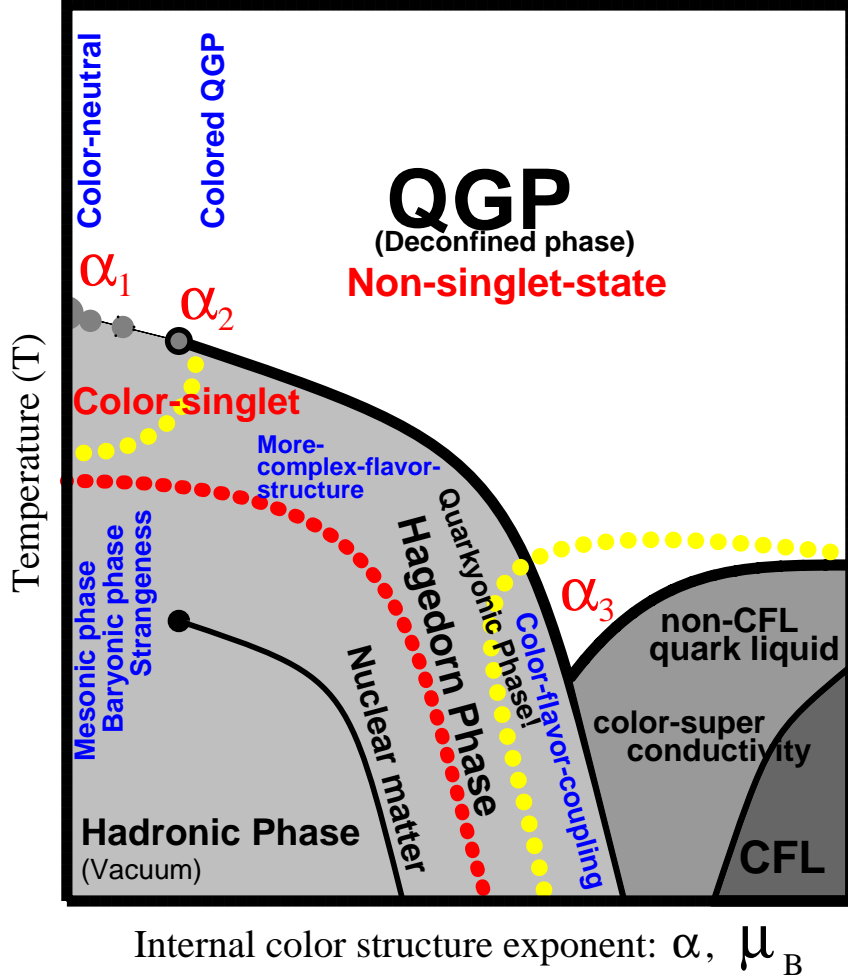


FIG. 3: (Color online) Same as Fig. (1). The order of the phase transition from the hadronic phase to the quark-gluon-plasma is shown to depend on the Hagedorn mass spectral exponent  $\alpha$ . The exponent  $\alpha$  is modified and increases with respect to  $\mu_B$ . The order of the phase transition is likely to be the first order, second order and higher order for the exponents  $\alpha_1$ ,  $\alpha_2$  and  $\alpha_3$  respectively. The quark-gluon plasma is likely to maintain the color neutrality one with the higher order phase transition at small  $\mu_B$  and high  $T \sim T_c$  before it switches to the true deconfined colored plasma when  $\mu_B$  increases. The exponent  $\alpha$  depends on the Hagedorn's internal color, flavor and configuration symmetries.

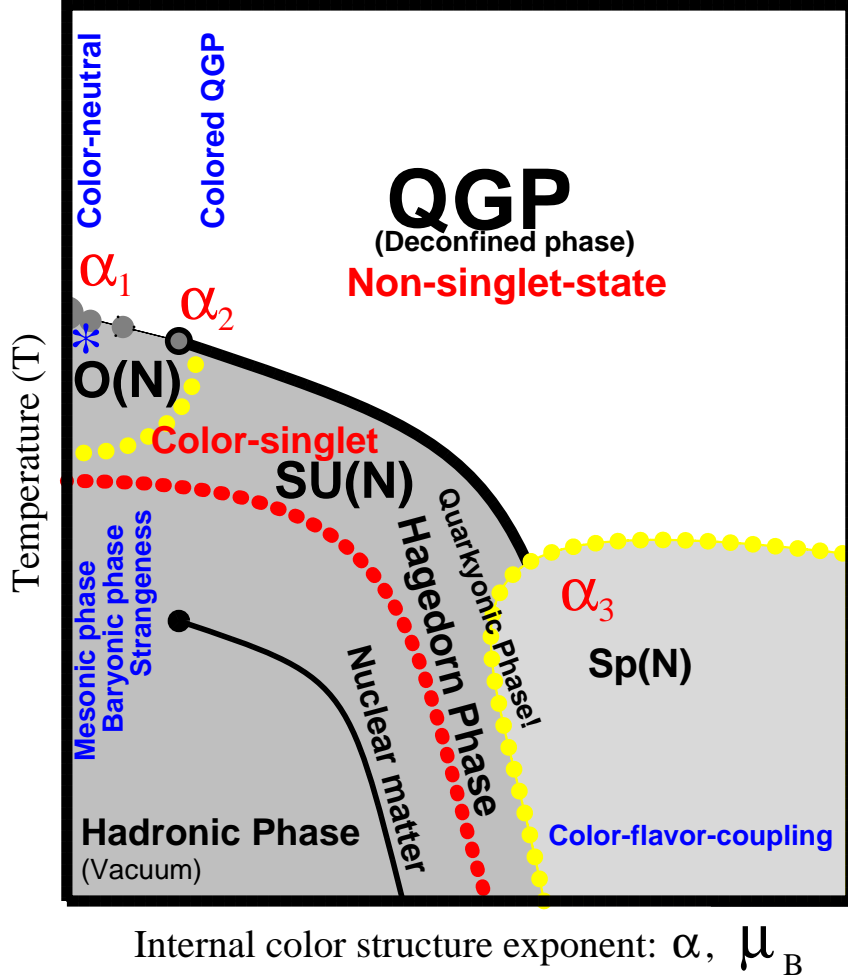


FIG. 4: (Color online) Same as Fig. (1). The complexity of the Hagedorn bag's internal structure is proportional to  $\mu_B$  and is inverse proportional to  $T$ . When  $\mu_B$  becomes sufficient large, the color and flavor degrees of freedom are coupled to each other and form  $Sp(N)$  symmetry group. The complexity of the color-flavor symmetry and space configuration symmetry increases as the system is cooled down and extremely compressed to large  $\mu_B$ .

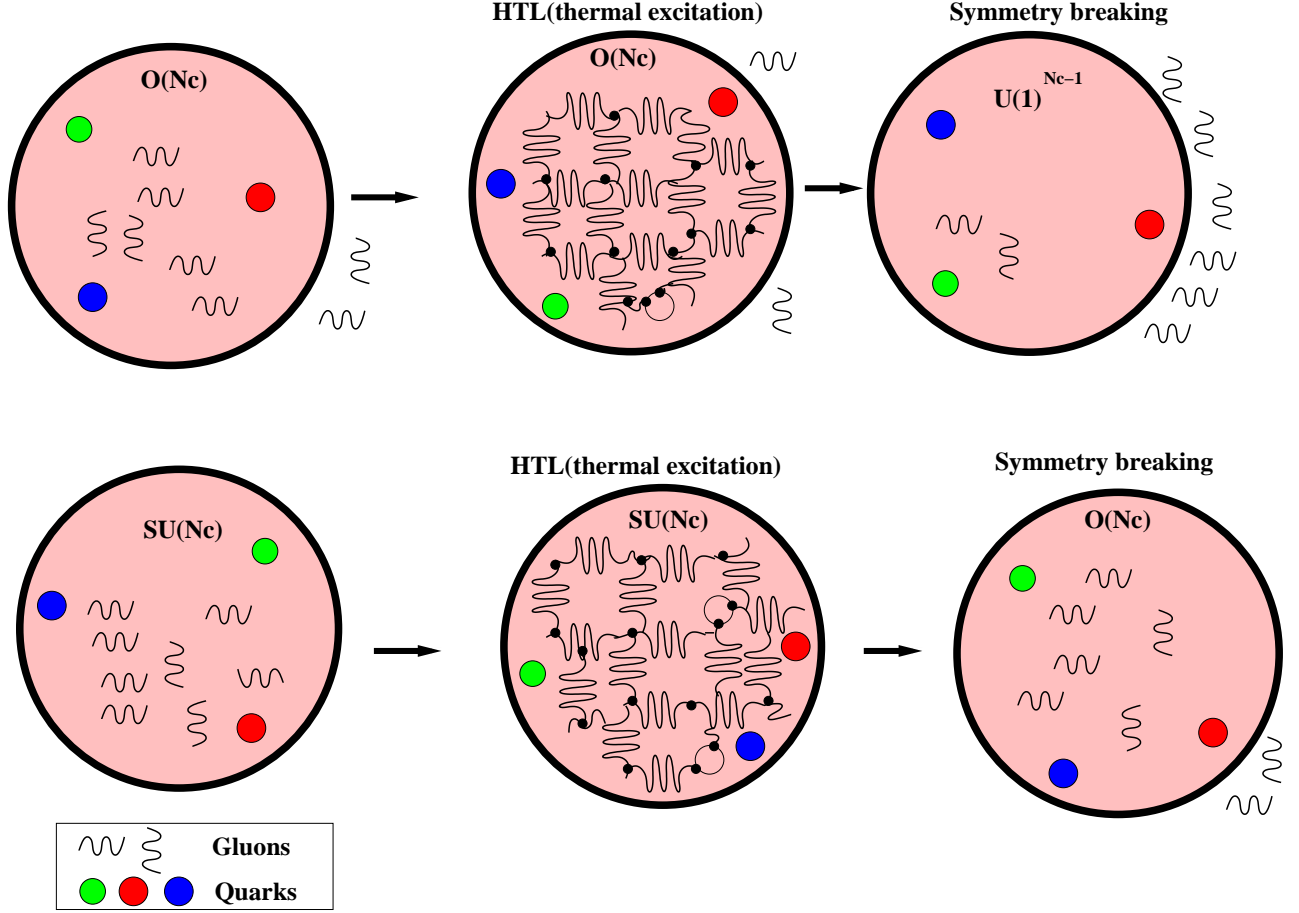


FIG. 5: (Color online) The Hagedorn's bag internal symmetry breaking from  $SU(N_c)$  to  $O(N_c)$  and eventually to  $U(1)^{N_c-1}$  in the dilute and hot nuclear matter. The quarks are represented by colored circles while the gluons are shown by short wavy lines. The hard thermal loop is expected to generate degenerate/non-degenerate gluon's Debye masses with vanishing/non-vanishing adjoint (mean-) fields  $\hat{A}^a$  depending on the medium. This mechanism is responsible for the symmetry transmutation in order to reduce to the constituent quark-gluon self-interactions and basically to maintain the quark confinement. The liberated gluons acquire finite masses ( $m_D^2 \propto g^2 T^2$ ) due to the Higgs phenomenon. In the present calculation, the liberated gluons are practically treated as an ideal gas of massless particles.